Universidade do Minho
Escola de Engenharia

José Miguel Gonçalves Ledo Belo da Costa

Optimization of filling systems for low pressure by Flow 3D

novembro de 2015

UMinho | 2015
José Miguel Gonçalves Ledo Belo da Costa Optimization of filling systems for low pressure by Flow 3D

Universidade do Minho
Escola de Engenharia

José Miguel Gonçalves Ledo Belo da Costa

Optimization of filling systems for low pressure by Flow 3D

Dissertação de Mestrado
Ciclo de Estudos Integrados Conducentes ao
Grau de Mestre em Engenharia Mecânica

Trabalho efectuado sob a orientação do
Doutor Hélder de Jesus Fernades Puga
Professor Doutor José Joaquim Carneiro Barbosa

novembro de 2015

DECLARAÇÃO

Nome: José Miguel Gonçalves Ledo Belo da Costa
Endereço eletrónico: joseledobelo@gmail.pt Telefone: 936831329
Bilhete de Identidade/Cartão do Cidadão: 13650073
Título da dissertação: Optimization of filling systems for low pressure by Flow 3D®

Orientadores:
Doutor Hélder de Jesus Fernandes Puga
Professor Doutor José Joaquim Carneiro Barbosa

Ano de conclusão: 2015
Mestrado Integrado em Engenharia Mecânica

DE ACORDO COM A LEGISLAÇÃO EM VIGOR, NÃO É PERMITIDA A REPRODUÇÃO DE QUALQUER PARTE DESTA TESE/TRABALHO.

Universidade do Minho, _____/_____/_________

Assinatura:

ACKNOWLEGMENTS

I express my deep gratitude and admiration
to Doctor Hélder Puga
for the constant motivation that passed me, the high scientific skills
and that it has and tried to pass on during this work.
His constant availability, your encouragement, your friendship, your confidence and your support
greatly contributed to the dissertation presented here.
My sincere thanks

To Professor Doctor Joaquim Barbosa
the constant availability, your encouragement, your friendship, your confidence and your support
greatly contributed to the thesis presented here.

To DEM,
the availability of all possible resources to this work.

I would also like to express my gratitude to a group of people, which encouraged me, doing better every day:
To CINFU particularly to Engineer Paulo Aguiar
the enormous availability and permanent advice throughout my scientific path, their assistance in the
experimental step was precious to the culmination of this work.

To Engineer Raul Truchado
the assistance given and high availability to meet my questions and having the critical spirit that
fostered the rapid developed in the short time that we were in contact.

To Engineer José Atilano
companion in this path, my thanks for all the cooperation, friendship and
to all conversations and discussions that helped me grow through the academic live
and for all the help invested in this work.
I wish you success

To João Viana
my thanks for all the support, cooperation, friendship
and for all the time and dedication invested in helping me throughout this path.

To my colleagues at the University of Minho,
i thank your companionship given in these academic live.
Highlighting those who followed me closely throughout this journey.

My parents and my grandparents
who contributed their efforts and support for the realization
to this personal goal. Without their help I wouldn’t be able to achieve this goal.
A special thanks to them.

To all,

Thank you

ABSTRACT

As part of the dissertation and bearing in mind the parameters in which the possibility of a choice of tutor and the subject to be addressed is established, the subject for development *'Optimization of filling systems for low pressure by Flow 3D* ®' was chosen. For this it was necessary to define the objectives to achieve and the methods to attain them.

Despite the wide range of software able to simulate and validate filling systems, Flow 3D® has been shown as one of the best tools in the market, demonstrating its ability to simulate with distinctive accuracy with respect to the entire process of filling and the behavioral representation of the fluid obtained. To this end, it is important to explore this tool for a better understanding of the processes involved and to serve as an exploratory basis for the simulation of filling systems, simulation being one of the great strengths of the current industry due to the need to reduce costs and time waste, in practical terms, that lead to the perfecting of the dimensioning of filling devices, which are reflected in delays and wasted material.

In this way it is intended to validate the methodology to design a filling system in low-pressure casting process, exploring their physical models and thus allowing for its characterization. For this, consider the following main phases: The exploration of the simulation software Flow 3D®; modeling of filling systems; simulation, validation and optimization of systems modeled by exploring the parameters of the models. Therefore, it is intended to validate the pressure curves under study and the eventual mining of the most relevant information in a casting analysis. The pressure curves that were used were obtained through the gathered literature and the practical work previously performed. Through the results it was possible to conclude that the pressure curve with 3 levels meets the intended purpose of a laminar filling regime and associated speeds never exceeding $0.5\ m/s$. The pressure curve with 2 filling levels has a more turbulent system, having filling areas with velocities above $0.5\ m/s$. The heat transfer parameter was studied due to the values previously obtained didn't corroborate the behavior of dissipation regarding to the casting. In this way, new values, more in tune with the casting process, were obtained. The achieved results were compared with those generated by NovaFlow & Solid®, which were shown to be similar, validating the parameters established in the simulations. Flow 3D® was proven a powerful tool for the simulation of casting parts.

Key-words: Low Pressure, Flow 3D®, Simulation, Foundry, Pressure-time relation

RESUMO

Como parte da dissertação tendo em mente os parâmetros onde está estabelecida e tendo em conta os moldes estipulados, permitiram a escolha do orientador bem como do tema a abordar. Optou-se pelo desenvolvimento do tema 'Otimização de sistema de enchimento para baixa pressão no software Flow 3D®'. Para isso foi necessário definir os objectivos a atingir e os métodos para alcançá-los.

Apesar da ampla gama de software capazes de simular e validar sistemas de gitagem, o Flow 3D® tem-se revelado como uma das melhores ferramentas do mercado, evidenciando a capacidade de simular com maior rigor no que respeita a todo o processo de enchimento de cavidades. Para tal, torna-se importante a exploração desta ferramenta para uma melhor compreensão das metodologias envolvidas e como base exploratória para a simulação de sistemas de enchimento, sendo a simulação um dos grandes trunfos da indústria atual, face à necessidade de diminuição de custos e de desperdício de tempo no aperfeiçoamento prático do dimensionamento dos sistemas de enchimento, que se refletem em atrasos e em desperdício de material.

Desta forma pretende-se validar uma metodologia de projeto dum sistema de enchimento através do processo de fundição de baixa pressão, explorando as capacidades e modelos matemáticos do Flow 3D®. Para isso, consideraram-se as seguintes fases principais: modelação, discretização do modelo; simulação, validação e otimização de sistemas modelados explorando os parâmetros dos mesmos. De forma a simular o enchimento da cavidade moldante, utilizaram-se curvas de pressão obtidas através da bibliografia e de trabalhos práticos previamente realizados. Pelos resultados obtidos foi possível concluir que uma curva de pressão com 3 patamares se encontra em regime de enchimento laminar, com velocidades associadas nunca superiores a $0.5\, m/s$ .Na curva de pressão com 2 patamares o regime de enchimento é mais turbulento, havendo zonas de enchimento com velocidades acima dos $0.5\, m/s$. O parâmetro de transferência de calor, full energy, foi estudado devido aos valores obtidos inicialmente não corroborarem com comportamento da dissipação face à fundição. Assim, foram obtidos valores consensuais com a prática de fundição. Compararam-se os resultados obtidos com resultados gerados pelo NovaFlow & Solid®, que se mostraram idênticos, validando deste modo os parâmetros relativos às simulações. O Flow 3D® revelou-se uma ferramenta poderosa face à simulação de elementos de fundição.

Palavras-chave: Baixa Pressão, Flow 3D®, Simulação, Fundição, Relação pressão-tempo

CONTENT

Acknowlegments iii
Abstract v
Resumo vii
Content ix
List of Figures xi
List of Tables xv
Acronyms and Abbreviations List xvii
1. Introduction 1
  1.1 Aim of the Dissertation 1
  1.2 Methodology of the Dissertation 2
  1.3 Layout of the Dissertation 2
  1.4 Scope of the Dissertation 3
2. State of the Art 5
  2.1 Low Pressure 5
    2.1.1 Advantages and Disadvantages 7
  2.2 Essential Parameters of the Low Pressure Casting 9
    2.2.1 Mold Temperature 9
    2.2.2 Pre-heating of the mold 10
    2.2.3 Temperature of Liquid Metal 10
    2.2.4 Pressure Needed to Pressurize the Molten Metal 10
    2.2.5 Stabilization Pressure 12
    2.2.6 Alloys Used in Low Pressure Casting 12
  2.3 CAE in Casting 13
  2.4 Computational Fluid Dynamics (CFD) methods 15
    2.4.1 Finite Difference Method 16
    2.4.2 The Finite Element Method 17
  2.5 Construction of the Model 18
3. Computational Modelling 21

- 3.1 Introduction 21
- 3.2 Governing Equations 21
- 3.3 Control Volume Approach 23
- 3.4 Volume-of-Fluid Method 26
- 3.5 Construction of the Geometric Model 28
- 3.6 Meshing 29
- 3.7 Boundary Conditions 31
- 3.8 Physical Models 32

4. Numerical Simulation 35
   - 4.1 Model Definition (CAD) 35
   - 4.2 Numerical Definition 37
   - 4.3 Modifications 41
   - 4.4 Final Simulations 47
   - 4.5 Software simulation comparisions 61

5. Conclusions and Future Prospects 63
   - 5.1 Conclusion 63
   - 5.2 Future Prospects 65

Bibliography 67

Attachment I – Boundary Conditions 71

Attachment II – Designação do Anexo II 73

LIST OF FIGURES

Chapter 1

Figure 1.1 - Design cycle 1

Chapter 2

Figure 2.1 - (a) example of low pressure casting system, (b) example of pressure curve 6
Figure 2.2 - Example of low pressure casting using sand molds 7
Figure 2.3 - Cycle of digital data... 14
Figure 2.4 - CFD software... 18

Chapter 3

Figure 3.1 - Cell representation of scalar and vector quantities 23
Figure 3.2 - Fractional area representation.. 24
Figure 3.3 - Example of cases where a single mesh block is not efficient.............................. 25
Figure 3.4 - (a) Example of linked blocks, (b) Example of nested blocks 25
Figure 3.5 - Interaction between fluids 26
Figure 3.6 - Representation of the VOF method 26
Figure 3.7 - TruVOF representation... 27
Figure 3.8 - (a) Geometric model, (b) Meshed model, (c)Favorized mode 29
Figure 3.9 - Application of the fixed points 30
Figure 3.10 - Errors from rough mash grids.. 30
Figure 3.11 - Mesh with open volume 31
Figure 3.12 - Symmetric boundary 31
Figure 3.13 - (a) Air entrainment parameters, (b) Bubble and phase change parameters........ 32
Figure 3.14 - (a) Gravity and non-inertial reference frame parameters, (b) Heat transfer parameters 33
Figure 3.15 - Viscosity and turbulance parameters.. 34

Chapter 4

Figure 4.1 - Measurement on Geometric model used in the simulation 35
Figure 4.2 - (a) Geometric model, (c) Flow 3D® model regarding different components (Blue – Hole, Red . Solid) 36
Figure 4.3 - (a) Part for final simulation, (b) section view (c) Flow 3D® model 36
Figure 4.4 - Methodology flowchart 37
Figure 4.5 - Solid properties from the sand mold 38
Figure 4.6 - (a)Favorized part with 7mm size mesh, (b) Favorized full model, with 11mm size mesh 39
Figure 4.7 - (a) Favorized part with smaller mesh size, (b) Favorized full model with smaller mesh size 39
Figure 4.8 – Simulated part with mesh of symmetric boundary conditions and pressure boundary condition in the entry of the molten metal 40
Figure 4.9 - Test curve pressure to obtain a fully functional simulation 41
Figure 4.10 – Simulation without the z max open volume 41
Figure 4.11 - Fill fraction graph of simulation without the z max open volume 41
Figure 4.12 - Pressure boundary condition to z maximum open volume 42
Figure 4.13 - Fill fraction with z maximum open volume 42
Figure 4.14 - Pressure simulation of z maximum open volume.. 42
Figure 4.15 - Model with virtual valve to simulate the permeability capacity of the mold enabling the output of gases to the atmosphere... 43
Figure 4.16 - Valve parameters used to simulate the permeability of the mold 43
Figure 4.17 - Fill fraction graph with model with virtual valve... 43
Figure 4.18 - Simulation with virtual valve to simulate the permeability of the mold 44
Figure 4.19 - Fill fraction graph with 2mm mesh size 44
Figure 4.20 - Simulation with 2mm mesh size.. 44
Figure 4.21 - (a) Favorized part with 4mm mesh size, (b) Favorized part with 2 mm mesh size 45
Figure 4.22 - Model with virtual valves to simulate the permeability of the mold regarding the entry zones of molten metal 45
Figure 4.23 - Simulation with valves 46
Figure 4.24 - Model with virtual valves in the extremities of the geometries to simulate the permeability of the mold promoting a more uniformed filling 46

Figure 4.25 - Pressure curve 1 47

Figure 4.26 - Fill fraction pressure curve 1 48

Figure 4.27 – Values of pressure contours for simulation of p-t (1): (a) values at 9.15s, (b) values at 10.14s, (c) values at 10.73s, (d) values at 20s 49

Figure 4.28 – Values of temperature contours using the uniform component temperatures heat transfer parameter for simulation of p-t: (a) values at 9.15s, (b) values at 10.14s, (c) values at 10.73s, (d) values at 20s 50

Figure 4.29 - Values of velocity magnitude contours for simulation of p-t (1): (a) values at 9.15s, (b) values at 10.14s, (c) values at 10.73s, (d) values at 20s 51

Figure 4.30 - Values of fluid flux for simulation of p-t (1): (a) values at 9.15s, (b) values at 10.14s, (c) values at 10.73s, (d) values at 20s 52

Figure 4.31 - Fill fraction pressure curve 2 53

Figure 4.32 - Pressure curve 2 53

Figure 4.33 - Values of pressure contours for simulation of p-t (2): (a) values at 3.80s, (b) values at 4.43s, (c) values at 4.81s, (d) values at 15s 54

Figure 4.34 - Values of temperature contours using uniform component temperatures heat transfer parameter for simulation of p-t (2): (a) values at 3.80s, (b) values at 4.43s, (c) values at 4.81s, (d) values at 15s 55

Figure 4.35 - Values of velocity magnitude contours for simulation of p-t (2): (a) values at 3.80s, (b) values at 4.43s, (c) values at 4.81s, (d) values at 15s 56

Figure 4.36 - Values of fluid flux for simulation of p-t (2): (a) values at 3.80s, (b) values at 4.43s, (c) values at 4.81s, (d) values at 15s 57

Figure 4.37 – New heat transfer parameters chosen to achieved temperatures validated with the bibliography 58

Figure 4.38 - Values of temperature contours using the full energy heat transfer parameter for simulation of p-t: (a) values at 9.15s, (b) values at 10.14s, (c) values at 10.73s, (d) values at 20s 59

Figure 4.39 - Values of temperature contours using full energy heat transfer parameter for simulation of p-t (2): (a) values at 3.80s, (b) values at 4.43s, (c) values at 4.81s, (d) values at 15s 60

Figure 4.40 – Comparison between software simulations (a) Flow 3D® simulation, (b) NovaFlow & Solid® simulation 62

LIST OF TABLES

Chapter 4

Table 4.1 - Initial conditions of simulation 37

Table 4.3 - Tested pressure curves 47

Table 4.2 - Initial conditons of simulation of pressure curve 1 47

Table 4.4 - Initial conditions of simulation of pressure curve 2 52

ACRONYMS AND ABBREVIATIONS LIST

Symbol	Definition	Unit
AF	Area Fullness	-
BEM	Boundary Element Method	-
CAD	Computer Aided Design	-
CAE	Computer Aided Engineering	-
CAM	Computer Aided Manufacturing	-
CAPP	Computer Aided Process Planning	-
CFD	Computational Fluid Dynamics	-
CNC	Computer Numerical Control	-
FAVOR	Fractional Area Volume Obstacle Representation	-
FDM	Finite Difference Method	-
FEM	Finite Element Method	-
FVM	Finite Volume Method	-
LPC	Low Pressure Casting	-
MRP	Manufacturing Resource Planning	-
STL	Stereolithography	-
VF	Volume Fullness	-
VOF	Volume of Fluid	-
	Roman symbols	
$(p\text{-}t)$	Pressure –Time	Pa/s
A_x	area vector on x axis	-
A_y	area vectors on y axis	-
A_z	area vectors on z axis	-
D/D_t	Operator of material derivative	-
V_f	Volume fraction	%
f_s	Solid phase fraction at the solidification stage	%
$\bar{t}$	Viscous stress tensor	-

D	Diameter of the riser tube	m
g	Acceleration due to gravity	m/s^2
H	Height difference between the surfaces of the molten metal ant the top of the riser tube	m
p	Pressure	Pa
Re	Reynolds number	Dimensionless
t	Time	s
v	Velocity of the molten metal	m/s
F	Forces	N
Ku	Drag	-
L	Latent heat	J/kg
$RSOR.(u/\rho)$	Accelerations caused by mass injection at zero velocity	m/s^2
T	Temperature	K
	Greek symbols	
∇	Nabla operator	-
μ	Dynamic viscosity	$Pa.s$
λ	Thermal conductivity	$W/(m.K)$
ρ	Fluid density	kg/m^3

1. INTRODUCTION

During the last years, the foundry industries have undergone major changes in their supplier profile, going from a simple subcontracting company to a provider of products and excellent technology services. This scenario, coupled with strong competition from the cast components market, makes smelters having the need to offer products and services with progressively better features, both visual and functional.

1.1 Aim of the Dissertation

The process of mold design in the foundry industry has long been based on the intuition and experience of foundry engineers and designers. To bring the industry to a more scientific basis, the design process should be integrated with scientific analysis such as fluid flow, heat transfer and stress analysis. In this sense, the design project is no longer part of the conventional analytical methods in which are fully grounded in the power of computer aided engineering (CAE), which has been optimizing the amount of time needed for design to an unparalleled level, in addition to integrating complex numerical models capable of modeling various parameters associated with the casting process.

Within these parameters, in the case of the results for the filling of the cavities, the prediction of the metal flow profile can be analyzed, as well as the temperature profile, speed and pressure. For the results associated with solidification, there is the solidification profile itself, predicting regions prone to the incidence of porosity, the final microstructure prediction, mechanical properties and residual stress.

Starting with the original design, a computer model is used to simulate the casting process. Given a set of criteria, defects can be predicted and modifications can be suggested to the original design. After several iterations of this design cycle, an optimum design, free of defects should be produced (Figure 1.1).

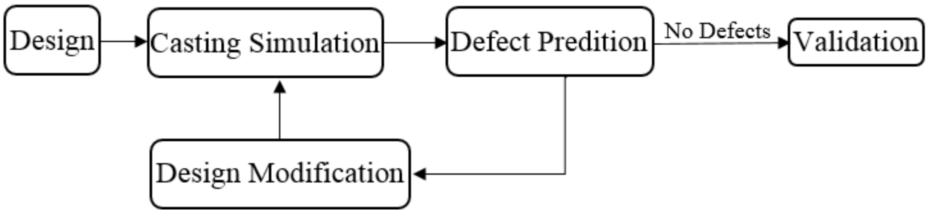

Figure 1.1 - Design cycle [1]

From this procedure, it will be possible to conclude whether a given mold design will produce a soundness casting, without having to discover this in the foundry through the usual trial and error process, which can be very tedious, time consuming and expensive. The performance of this design cycle is based on the accuracy of the casting simulation and the legitimacy of the defect prediction criteria.

With this new mindset level it has been possible to minimize manufacturing time, assuring the final quality of components, which leads to a great saving of production resources, both at the level of the associated costs and in the equipment maintenance. In this dissertation the analyzed material was the aluminum A357 with an initial temperature of fluid of 700ºC.

1.2 Methodology of the Dissertation

To the investigation of models that can be used to validate the process, two methods can be of use. The first is experimental, and consists of the investigation of the physical process to establish thermophysical data and defect criteria. The other method, used in this dissertation, involves the construction and testing of a computer model. This is achieved with the following strategy:

- A literature review to examine important contributions and to establish the current state of process;
- Examination of existing computer models to determine their suitability;
- Construction and/or modification of a computer model;
- Improvements to the computer model to increase speed and accuracy;
- Theoretical validation and testing of the computer model.

1.3 Layout of the Dissertation

This essay’s content follows a structure going from the general to the particular, enabling the reader a progressive and integrated view of the various related topics. An introduction is presented in Chapter 1, in which the approach and objectives of the study are broadly established. Chapter 2 is about the theoretical basis of the work, tracing the author’s line of thought, explaining what is low pressure casting, characterizing the process in general, introducing the importance of CAE in to casting and the importance of the simulation process in the foundry industries. Chapter 3 deals with all the general information behind the used software, showing the routine equations, how it works, and the possible characterizations of the models to make a working simulation. In Chapter 4, the entire process in the creation of the simulation for this dissertation is described and the model, the boundary conditions, the modified parameters and the encountered problems. Chapter 5 present the validation of the simulations and is performed the comparison of simulations of the same model simulated in NovaFlow®. The conclusions and the future prospects are allocated in Chapter 6. Subsequently, the consulted and cited references used throughout the document are presented, prior to the attachments. Thus, it is expected that the reader can see clearly the logical order chosen in the problem domain under study.

1.4 Scope of the Dissertation

The scope of this dissertation has been the investigation of the pressure map obtained and the analysis of the fluid flow behavior, thus it is possible to control the velocity regime, preventing the entrapping of air that causes damage to the castings. In this project it was planned to develop skills by using the software Flow 3D®, in order to explore the simulation filling system design in low pressure casting process. More specifically, it aims for a better understanding of mesh and the simulation of computational models using different physical models. With the execution of this project it is intended to achieve the following objectives:

- Describe the velocity profile during the filling of mold cavity;
- Establish pressure and temperature parameters to perform the filling of mold cavity.

Since one of the pillar basis of this work is the low pressure casting there is the need to specify how it works in order to clarify what differs when comparing with other casting processes. Thus the process was characterized by addressing the essential parameters for its occurrence and to what extent these parameters affect the process execution.

The limitations in this study were mostly the lack of literature on the Flow 3D® software and the process of developing the simulation being rather long-lasting, having to explore it. There is also a lack of literature about the process of low pressure casting, and very few studies can be found concerning the operation of low pressure casting and the study of the setting of the pressure-time (*p-t)* curve during filling and the parameters to create the simulation are even scarcer. As a solution, an iterative approach was used, in order to find some parameters. This method was chosen since the study of the physical process is not economically viable. Another limitation was of technological order, not having access to sufficient computational power to meet the forecasted data.

2. STATE OF THE ART

2.1 Low Pressure

Metal casting has always been one of the most important and widely used manufacturing processes. Advantages inherent to castings such as design, metallurgical features and to the casting process itself make them superior to other manufacturing methods. Egyptians used solidification processing to create near net-shaped components 5100 years ago [2]. As this processing developed, it markedly expanded with the industrial revolution and the advancement of technology through the 20th century. Today, a variety of molding processes and melting equipment are available to cast different types of metals and alloys in foundries [2].

The increasing number of applications and products is evidence of the success of aluminum alloys for casting. This is probably one of the most dynamic areas within the manufacturing universe. The advantages associated with the use of aluminum alloys, such as low weight, good mechanical performance, good corrosion resistance, etc., are recognized as the driving force for the introduction, on one hand, of new applications and manufacturing systems and, secondly, of the development of new processing solutions.

Several processes currently compete to achieve an economically and technologically advantageous production of cast aluminum alloys [3].

Among the most interesting processes, the low pressure casting is a "near net-shaped" process, relevant thanks to its special features, allowing in many cases an excellent compromise between quality, cost, productivity and geometric feasibility. Even though an old process (the first patent on the molten lead alloys, is deposited in England in 1910), significant industrial application started thirty years ago [3].

Nowadays, it is adopted for casting aluminum alloys and magnesium based alloys. A low-pressure casting machine usually includes a pressurized melt furnace located below the die table with a feeding tube running from the furnace to the bottom of the die. The filling of the cavity is obtained by forcing (by means of a pressurized gas, typically ranging from 0.1 to 1 bars [4,5]) the molten metal to rise into a ceramic tube (which is called stalk), which connects the die to the furnace (Figure 2.1(a)). The gating system is usually positioned in the middle of the casting, which corresponds to the center of the crucible, in order to guarantee uniform pressure and, therefore, flow distribution [3,4,6,7].

The surface of molten metal in the furnace is pressurized by a dry protective gas at relative low pressure to overcome the difference of metallic pressure between the die and the surface of the molten metal. The liquid is then forced to rise through the riser tube and that consequently feeds the die cavity. When the die cavity is full, the pressure is increased , depending on the material of the mold, to pressurize the casting and improve the feeding of shrinkage during solidification (Figure 2.1 (b)) [3,4,8].

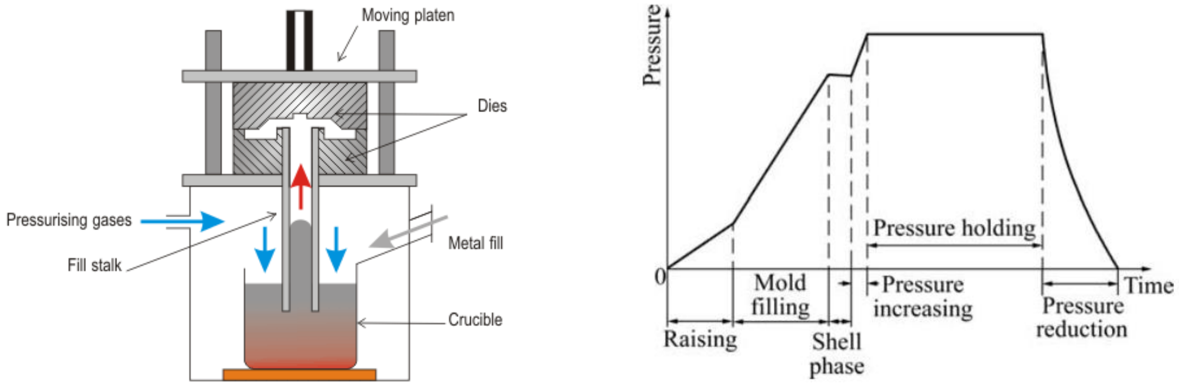

(a) **(b)**

Figure 2.1 – (a) example of low pressure casting system [6], *(b) example of pressure curve* [9]

Once the die cavity is filled, the overpressure in the furnace is removed, and the residual molten metal in the tube flows again towards the furnace. The various parts of the die are then separated, and the casting is finally extracted. Specific attention has to be applied to the design of the die to control, using a proper cooling circuit, the solidification path of the alloy. The massive region of the casting has to be the last one to solidify and must be placed around the stalk, which acts as a “virtual” feeder and allows one to avoid the use of conventional feeders - this way it can get yields of the alloy used, close to 95%, which becomes significantly high, when compared with other processes [3,10].

Low pressure casting (LPC) process allows the optimization of the mold filling channels which leads to a reduction or even elimination of the feeders. With this, reduce the amount of additional finishing operations of the cast [3]. The rapid solidification rate associated with the low-pressure casting allows the casting of parts with finer grain size, smaller interdendritic spaces, and leads to an increase of mechanical properties [8]. The molds normally are made of metal, however, there is the need to apply diverse refractory coatings on the surfaces in contact with the molten metal to avoid its adhesion to the mold, thereby minimizing the loss of temperature during the filling and control solidification [5].

In the low pressure process fully produced sand molds can be used (chemically bound) (Figure 2.2), however, it is used only in very specific conditions. Many castings now

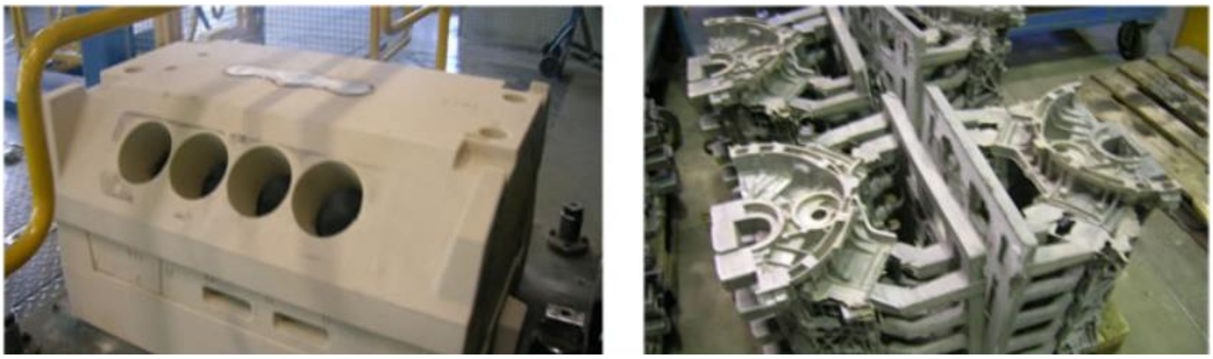

Figure 2.2 - Example of low pressure casting using sand molds [5]

produced by sand casting or the casting process by gravity can also be casted by the low-pressure process [5].

The low pressure casting presents two variants. The first, is called vacuum casting and is in everything else similar to the low-pressure casting process [11]. The metal is poured inside the cavity not by applying a greater pressure in the chamber containing the crucible, but by decreasing the pressure in the mold cavity through the creation of vacuum.

The second variant is called the Griffin method of casting in permanent molds of graphite, having been developed by "Griffin Wheel Company of Chicago". This company produced wheels for trains, a product whose requirements in terms of mechanical properties were very high. The high steel melting temperature material from which they were formed, made the metallic permanent molds not suitable. The foundrymen of the company then tested the use of graphite molds, given the characteristics of thermal conductivity, stiffness and swelling/shrinkage of this material. Later it was found that the molds suffer erosion very quickly due to the leaking of. Casting under low pressure was used, eventually leading to what is now the Griffin method: essentially a casting method in permanent molds of graphite by low pressure [11].

2.1.1 Advantages and Disadvantages

The low pressure casting process has several advantages over conventional casting processes. The castings have almost a 95 % yield and therefore are much less wasteful of aluminum. The low pressures allow sand cores to be used for interior passages, and the casting has a better final shape and surface finish due to the use of the permanent mold [3,10,11].

There is also a much greater degree of control of the filling and solidification rate of a casting using this process, than in conventional gravity or high-pressure die casting [2,9]. To sum up these are the main advantages according to [3–5,7,10,11]:

- Improved mechanical properties;
- Filling is less turbulent, possible to obtain laminar regimes, minimizes aspiration of air and oxidation;
- Allows the precise control of the mold filling time;
- Minimizes general finishing operations (provides low levels of scrap);
- Allows use of sand molds and sand cores without the danger of destruction;
- Saves time regarding to the CAD (Computer aided design) process because it is not needed to model all the runner system;
- Allows castings without porosities originated from turbulence regime;
- Easy automation of the casting process;
- There is a reduction of needed material in the absence of the feeding channel.
- The products of improved mechanical, physical and operational properties are achieved;
- Castings solidify faster and this provides a higher productivity in comparison with other casting methods;
- Possibility of full automation of the entire casting process ensuring a high quality of products, possibly allowing quick adjustments and equipment increases, elimination of the human factor during the production process and the possibility of visual control and electronic transfer of technical data.

Despite its many advantages, low-pressure casting is not yet fully appreciated [12]. These are the main disadvantages according to [5,10–12]:

- High cost of equipment (a process not suitable for small series);
- The costs of maintenance of the molding feeding system (from the crucible to the casting itself);
- Difficult access to the metal in the crucible stored (e.g., for inspection or treatment)
- Need to interrupt the process for replenishing supplies;
- Although other metals may be casted using low pressure casting, this process is practically limited to the use of light alloys;
- The need of optimization;
- High initial cost of investment;
- Lack of understanding of the low pressure process.

2.2 Essential Parameters of the Low Pressure Casting

There are several parameters that influence the process of low pressure casting, such as the pressure in the filling, the velocity of the liquid, stabilization pressure, pouring temperature, thermal gradients, which are essential as they establish the direction of the solidification process, among others. Some parameters will be addressed in the next subchapter.

2.2.1 Mold Temperature

An optimum mold temperature is a temperature that will produce a casting in good conditions and in the shortest time. If the mold temperature is too high, the casted part becomes too brittle for the extraction without irreparable damage like the mechanical properties and the finishing of the part. When the mold temperature is too low the feeding is inhibited, which usually results in shrinkage, heat cracks and adhesion of the cast to the mold and to the cores. In more severe cases clogging and consequent stoppages of the production cycle may even occur. Factors influencing the temperature of the mold include (according to [11]):

- Pouring temperature: The higher it is, the higher the temperature of the casting mold must be;
- Cycle frequency: the faster the operation cycle, the higher the temperature mold;
- Volume of casting: the mold temperature increases as the weight of the molten metal increases;
- Shape of the cast: large sections insulated, cavities of the core and sharp edges not only increase the overall temperature of the mold, but also produce unwanted thermal gradients;
- The thickness of the solids such as the cast, in which the temperature of the mold increases as the thickness of the cast’s wall increases; the walls of the mold should be thicker when the temperature and the thickness of the coating of the mold decreases, also considering also that the temperature of the mold decreases as the thickness of the coating of the mold increases.

2.2.2 Pre-heating of the mold

In many foundry operations, the molds are pre-heated approximately between 200-350ºC. This practice minimizes the number of unacceptable castings produced during the initial phase of the production process. The mold can be pre-heated by direct exposure to a flame or through a muffle, which is not always practically possible due to the dimensions of the mold [11].

2.2.3 Temperature of Liquid Metal

The casted parts of the permanent mold are generally done with a metal which is maintained within a relatively tight temperature range. This range is established by the composition of the casted metal, the cast wall thickness, size and weight of the cast, cooling method of the mold, type of coating on the mold and feeding system used. If the casting temperature is lower than the ideal, the mold cavity will not be filled, the feed system will solidify before the last part of the casting process and the thin sections will solidify too fast and will stop the directional solidification [11].

Low casting temperature, results in stopping the production cycle, poor finishing and heat cracks. Sometimes only a small increase in the casting temperature is necessary to prevent these cracks. A high temperature casting causes contractions in the casted part and warpage of the mold, which leads to loss of dimensional tolerance. In addition, variations in metal composition may develop if the molten metal has components that become volatile at high casting temperatures. High casting temperatures also increase the solidification time (thereby decreasing the rate of production) and often decrease the life of the mold [11].

2.2.4 Pressure Needed to Pressurize the Molten Metal

A crucial part of the LPC operation is the control of the propelling pressure in the crucible to ensure a laminar flow of molten metal through the feeding tube into the mold. If the filling of the die is not properly controlled, the casting will suffer from filling related defects such as short fills or gas porosity. The current practices rely on the experience of casting engineers and the conscientious step of trail-and-error. The pressure required to fill a casting in the LPC process can essentially be separated into two stages [8,13,14]:

I. The first stage is to apply pressure to force the molten metal to rise through the feeding tube in a non-turbulent way to the gate of the casting mold. This varies from casting to casting, depending on the metal level and the volume of metal transferred. The pressure required is relatively easy to calculate applying Pascal's principle, $p = \rho g H$ where ρ is the density of the molten metal, p is the pressure, g is the acceleration due to gravity and H is the height difference between the surfaces of the molten metal and the top of the riser tube. H is a variable, since the level of the molten metal in the crucible keeps lowering as the casting proceeds. One question that needs to be addressed is how fast the molten metal needs to be in order to be forced to flow in the riser tube. The principle adopted is that it should be as quick as possible without causing disturbance of the fluid.

It is known that the fluid flow can be considered as laminar in a tube when Reynolds number (*Re)*, is less than 2100. To calculate *Re*, the following equation can be used (2.1):

$$Re = Dv\rho/\mu \tag{2.1}$$

Where D is the diameter of the riser tube, (m), v the velocity of the molten metal in the riser tube (m/s) and μ is the dynamic viscosity of the molten metal ($Pa.s$). The flow of molten metal in the tube needs to be non-turbulent, but not necessarily laminar, to avoid entrapping gas [14]. Secondly, the condition for laminar flow to be 2100 is for the fluid that flows in a pipe in a horizontal manner. In the low pressure casting process, the molten metal fills the riser tube in a vertical way and from the bottom. From industrial experience, it is known to be optimal to fill a riser tube of 50 cm in length and 9 cm in diameter in approximately 5 s: this is a rising velocity of 10 cm/s. With the properties of the molten aluminum, the Reynolds number can be as high as 21000 [14].

II. The second stage is the additional pressure required to push the molten metal into the die cavity to fill the cavity in a way that does not create much turbulence or entrap gas. The conventional principle is to have the molten metal flowing as slowly as possible, on the basis of reducing turbulence. This has the disadvantages of low productivity and possible premature solidification, which results in failure of the casting. It is not necessarily true that slow filling is always beneficial to the quality of the casting in terms of gas entrapment. The pressure required in the second stage is more complex since the desired filling patterns actually depend on the shape of the individual casting and can be determined by simulation [8,14].

Depending on the geometry of the casting, a favorable flow pattern should be determined by the engineer. In order to do this, the engineer can first divide the casting into several parts depending on its geometric characteristics and the various mechanical properties required for the different parts of the casting. He then can decide which part should be filled first, which part is next, and so on. Thus the most important decision should be to determine how quickly or how slowly each individual part should be filled [7,12].

Through the aid of a mold filling simulation system, he'll be able to decide whether the chosen gate velocity is modified and the flow pattern is simulated again until a desirable flow pattern is obtained. It is important to have in mind that aluminum oxide film on the surface is entrained into the bulk aluminum melt at a velocity greater than 5m/s producing major damage to the castings, so by using LPC it is possible to control this parameter and establish a relation between the exerted pressure and the velocity of the metal [15]. The process is repeated until the whole casting is filled. The engineer can examine the filling pattern, under the given gate velocity, to see if it is desirable or not. If not, a new gate velocity can then be set and the calculations resumed. The process is iterated until the whole casting is filled. Then an ideal relation between gate velocity and time can be obtained during the filling of the LPC. While calculating the filling pattern and the velocity profile, the required pressure at the gate can also be computed. With the combination of the stages I and II, during the filling of the casting, the *p-t* curve, can be obtained.[8,14].

2.2.5 Stabilization Pressure

A certain amount of pressure must be maintained after the cavity is filled until the metal solidifies in order to prevent shrinkage and produce the casted part. The stabilizing pressure time is another important parameter in the process. It can be determined with the aid of a simulation of solidification, to ensure that the molten metal is completely solidified before it solidifies in the riser. Subsequently the pressure is lowered that blockage of the riser doesn't occur [8,16].

2.2.6 Alloys Used in Low Pressure Casting

Aluminum alloys are the alloys most commonly used in LPC and the magnesium ones are the less used [11]. The practical sizes for permanent mold vary according to the material being cast, the required number of parts and their configuration. The parts produced by this process, although they can be very heavy, typically lie in the range of between 0.5kg and 50kg.

Some characteristics about the alloys, are going to be addressed, according to [11]:

- Aluminum alloys: have already been casted in permanent molds, for big series and parts weighing more than 70kg. Moving the molds consists in resorting to the use of mechanical devices. However larger parts can be produced.
- Magnesium alloys: despite its poor flow rate or casting rate, it has been used in foundries with permanent or semi-mold to produce relatively large and complex parts.
- Copper alloys: casting parts in copper alloys in a permanent mold weighing over 10 kg is rarely suited.
- Gray cast iron alloys: the production of parts in cast iron alloys in permanent mold is rarely practiced when they weigh over 15 kg.

2.3 CAE in Casting

Computer simulation of casting processes has been utilized since the early 1970's as a means of predicting solidification shrinkage in large castings. Since then, the capabilities and speed of simulations has grown tremendously to the point where nearly every detail of the casting process can be simulated. From computer simulations, process variables can be systematically adjusted without expensive prototyping and unnecessary production interruptions, resulting in increased development efficiency and new product deployment [17]. With the evolution of the 3D CAD programs, modelling has become more accessible for the designer. This means that modelling does not take much more time than just making the drawings and gives much more applications to the model. Simulation is just one application of 3D modelling [18].

Besides this, it has been estimated that about 90% of the defects in components is due to mistakes done in design and only 10% because of manufacturing problems. It has been also calculated that the costs to change the design are ten times higher in the next step of the design and manufacturing process. Thus all the methods and tools to ensure the result of the design will affect significantly the total manufacturing costs [18].

Refinement of design and increasing demands for better products have caused both designers and manufacturers to see how the computer might be used to aid them in their problems. Computers have now entered into the foundry engineering. The designers, using their experience and knowledge, produce projects and instructions, for manufacturing of the products based on the design specifications and the available installations and operators [19].

Consistent designing and planning require knowledge of casting processes and experience. Several consultations can be made in just one day, instead of first sending the drawings by mail and then organizing meetings between the parties to discuss the solutions. Both parties can point out the problems through the simulation results, which are easy to interpret [18]. This has led to the development of computer aided process planning (CAPP) systems, developed as a link between design and manufacturing, filling the existing gap between CAD and computer aided manufacturing (CAM) [20]. In this "digital factory", manufacturers, their suppliers and partners simultaneously work on the same numerical prototype (Figure 2.3), allowing for continuous improvement in design and immediate decision-making [21].

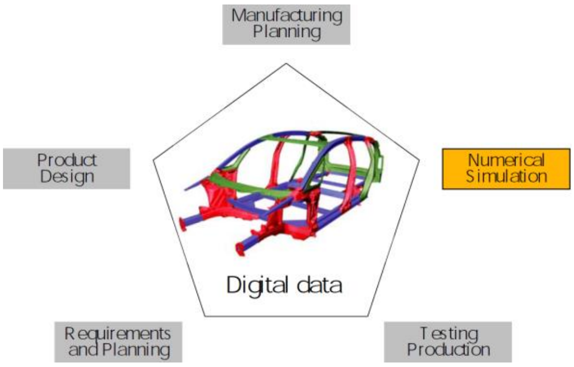

Figure 2.3 - Cycle of digital data [21]

CAPP allows the user to develop an integrated structure that deals with the flow of information between CAD, CAM, manufacturing resource planning (MRP) and CNC activities within the company. The main objective is the realization of a computer-aided system to help, automatically select and finally define the parameters of foundry models. In the applied methodology, the steps are divided into three parts: knowledge acquisition, the activity modification and finally development and implementation of the tool [20].

This "extended enterprise" marks a revolutionary departure from the time consuming and costly trial-and-error processes of physical prototyping [21]. Practical "Trial and Error" experiences are usually expensive and slow. Besides, the foundry process is a “black box”, where it is not possible to look inside. The use of simulation allows the foundrymen to understand the processes better. By computer simulation of the casting process, the flow of the molten metal in the cavity, the heat transformation, the solidification, grain formation, shrinkage and stress evolution can be visualized. The details are seen on the computer in graphical form, which helps the designers to visualize the defects in the process design, to analyze the causes of the defects (such as hot tears, shrinkage porosities, cold shuts etc.) [22].

This way, defects can be foreseen, even before the beginning of the mold construction. The process limits become visible and robust process conditions can be determined, avoiding that small process variations that affect the quality of the casting [23].

Modernization is the only key to improve casting quality and productivity. Due to the entry of computers in foundries, fatigue and strain on workers and staffs have been considerably reduced during working hours and work culture has improved tremendously. Improved work culture can lead to a sense of participation, involvement, and creativity [19].

With this new mindset, it has been possible to minimize manufacturing time, assuring the final quality of the components, which leads to a great saving of production resources, both at the level of the associated costs and the equipment maintenance, having as consequence a satisfied customer [19].

2.4 Computational Fluid Dynamics (CFD) methods

Computational fluid dynamics is the branch of fluid dynamics providing a cost-effective means of simulating real flows by the numerical solution of the governing equations. The governing equations for Newtonian fluid dynamics, namely the Navier-Stokes equations, have been known for over 150 years. There is a large number of commercial CFD packages in the market nowadays and CFD has established itself as a useful analysis and design tool. In addition, there is a large number of research and public domain CFD programs. CFD techniques have emerged with the advent of digital computers. Since then, a large number of numerical methods were developed to solve flow problems using this approach. The purpose of a flow simulation is to find out how the flow behaves in a given system for a given set of inlet and outlet conditions [24]. The basic concept of CFD methods is then to find the values of the flow quantities at a large number of points in the system. These points are usually connected together in what is called numerical grid or mesh. The system of differential equations representing the flow is converted, using some procedure, to a system of algebraic equations representing the interdependency of the flow at those points and their neighboring points. With the development of fast and validated numerical acquires, and the continuous increase in computer speed and availability of cheap memory, larger and larger problems are being solved using CFD methods at a lower cost and quicker turnaround times. In many design and analysis applications, CFD methods are quickly replacing experimental and analytical methods [24].

A classification of the numerical solution of three dimension advection-diffusion equations is based on the discretization method by which the continuous mathematical model is discretized in space, i.e., converted to a discrete model of finite number of degrees of freedom [25]:

- Finite Element Method (FEM);
- Boundary Element Method (BEM);
- Finite Difference Method (FDM);
- Finite Volume Method (FVM);
- Spectral Method;
- Mesh-Free Method.

Many author state that there are mainly two methods, FEM and FDM for numerical simulation of the casting processes [25,26], however the FVM is starting to gain more users. The most used methods are explained as follows:

2.4.1 Finite Difference Method

The FDM is the most popular method used for the discretization of differential equations. It is the simplest method to apply, particularly on uniform grids. However it requires high degree of mesh regularity. The mesh needs to be set up in a structured way where mesh points should be located at the intersection points of families of rectilinear curves [25]. The discretization is based upon the differential form of the partial differential equations to be solved. Each derivative is replaced with an approximate difference formula (that can generally be derived from a Taylor series expansion) [28]. The computational domain is usually divided into hexahedral cells (the grid), and the solution will be obtained at each nodal point. The FDM its clear to understand when the physical grid is Cartesian, however through the use of curvilinear transforms, the method can be extended to domains that are not easily represented by brick-shaped elements. For the discretization results in a system of equation of the variable at nodal points and for a solution is founded, the result is a discrete representation [28]. This method is difficult to use when faced with complex geometries. For this reason, this method is limited to practical applications and only a very small number of engineering codes rely on this method [25].

Nonetheless, the simplicity of the method allows us to explore the properties of various numerical discretizations and compare their degree of accuracy. It also allows us to have a better comprehension of numerical procedures. Additionally, for solution procedures which require higher order derivatives or high order of accuracy, this method can be better suited than other methods despite the limitation of mesh regularity [25].

2.4.2 The Finite Element Method

The FEM is based on the so called 'Method of Weighted Residuals'. This is a mathematical method for solving ordinary and elliptic partial differential equations via a piecewise polynomial interpolation scheme which was developed between 1940 and 1960, mainly for structural dynamics problems. This was extended later to the field of fluid flow [25,29]. Put simply, FEM evaluates a differential equation curve by using a number of polynomial curves to follow the shape of the underlying & more complex differential equation curve. Each polynomial in the solution can be represented by a number of points and so FEM evaluates the solution at the points only. A linear polynomial requires two points, while a quadratic requires three. The points are known as node points or nodes. There are essentially three mathematical ways that FEM can evaluate the values at the nodes, there is the non-variation method (Ritz), the residual method (Galerkin) & the variation method (Rayleigh-Ritz) [29]. This method has a distinct advantage over the FDM in the fact that it allows for naturally handling complex arbitrary geometries as it can be easily applied using irregular grids of various shapes [24]. It also provides a set of functions that gives the variation of the differential equations between grid points, whereas, FDM provides information for the values at grid points only. Nowadays, the FEM has been put in an engineering rigorous framework with precise mathematical conditions for existence, convergence and error bounds [24]. The FEM allows a variety of element shapes, for example, triangles, quadrilaterals in two dimensions and tetrahedral, hexahedral, pentahedral, and prisms in three dimensions. Each element is formed by the connection of a certain number of nodes, with the number of nodes in an element depending on the type of the element [25].

The FEM uses body fitted computational grids leading to a more accurate representation of melt/mold interface as compared to FDM. The FEM has the ability to handle complicated geometries (and boundaries) with relative ease. However, FEM required higher memory resources for calculations and required time consuming manual intervention and the usage of special generators for building 3D meshes. On the other hand, FDM offers ease of mesh generation due to the structured nature of the mesh and the use of fewer memory resources as compared to FEM. However, FDM often requires fine grids to describe geometries to reduce errors associated with the “stair-step” representation of curved boundaries [26].

Following there are some examples of software used for casting simulation (Figure 2.4):

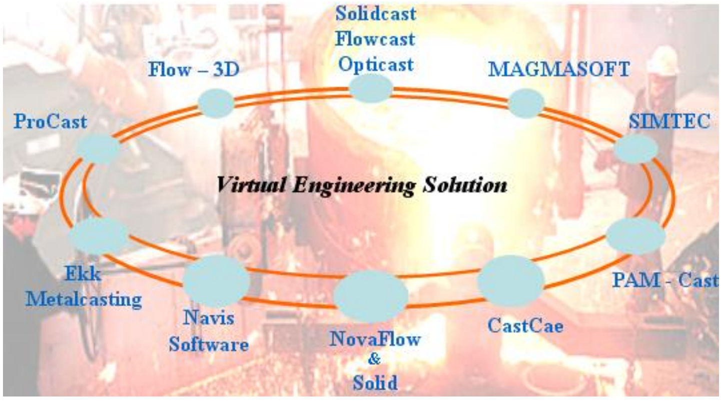

Figure 2.4 - CFD software [30]

In the examples of software Ekk Metalcasting®, Procast®, SIMTEC®, Solidcast®, Flowcast®, Opticast® are all governed by FEM and CastCae®, Flow 3D®, MAGMASOFT®, Mavis®, NovaFlow & Solid® are governed by FDM. With CAM-Cast® is possible to use both methods [30]. It is important to highlight that some software has packs that allow for the use of different methods in addition to those commonly used.

2.5 Construction of the Model

The construction of a geometric model can be broken into several evolutionary stages. During its construction, a number of assumptions can and must be made. These assumptions can be made, in light of our understanding, from the physical processes that are involved in the creation of the final part and the characteristic wanted for the same. Once the geometric model has been validated, it can be used to perform simulations [1].

The simulation modeling of the mold and the final part is an extremely important element in the success of the production parts. The study of the thermal fluid allows the creation of a simulation model of the part, making it possible to optimize the production process for companies, having the ability to get better quality products and get a much higher production output. The simulation model allows the engineer to evaluate the dynamic behavior of the molten fluid at various stages of the process and analysis [1]:

- The turbulence effect, that can facilitate the formation of oxides and inclusions;

- Vortex causing air drag;
- Sudden falls of temperature in the flow front, causing the appearance of discontinuities.

It will also analyze the dynamics of the solidification process associated with the transient heat retained by the mold in relation to [8,10,19]:

- Shrinkage;
- Porosity;
- Overheating of the mold which is a major cause of dimensional instability, causing difficulty in the removal of the part, reducing the molds life;
- The efficiency of the cooling channel, that affects the directional solidification;
- The time taken by each stage of the cycle in order to maximize productivity;
- Dimensional quality;
- Uniformity of the mechanical properties and microstructure.

Using micro structural non-ferrous models, specific to aluminum, is also possible to control [19]:

- Phase transformations during solidification to predict the secondary dendrite spacing;
- Microstructure and local mechanical properties for each phase.

The simulation of the production process allows the foundry industry to reduce waste and to optimize the molds, easily changing geometry and process parameters, to achieve a more efficient filling, solidification and cooling phases. The advantages of using virtual simulation during the design phase are numerous and include [8,10,19]:

- Waste reduction;
- A reduced number of necessary physical prototypes;
- Less design changes after the initial production;
- Increased productivity;
- Reduced time to market;
- Reduced raw materials used, reduced labor and energy required;
- The ability to have a full virtual and integrated model in which, the resultant information from the production process (a state of tension, microstructure and mechanical properties of the part) is passed to the finite element code to test the structural integrity [19].

3. COMPUTATIONAL MODELLING

3.1 Introduction

For low pressure simulation Flow 3D® software was used, which has been shown as one of the best tools on the market, proving its ability to simulate with great accuracy regarding the entire process of casting and the behavior representation of the fluid obtained. The software solves three-dimensional fluid-flow problems using the finite different approximation. The two equation k-epsilon model are used to solve the turbulent properties of the flow. The Navier– Stokes equations coupled with the energy equation allows the software to achieve an accurate solution for turbulent metal flow undergoing solidification [7].

To this end, the study of this tool is vital, for a better understanding of the processes, being the simulation one of the great strengths of the current industry due to the need to reduce costs and time wasted on practical improvement of the systems methodology (leading to delays and waste material).

3.2 Governing Equations

The governing equations are expressed in the Cartesian coordinate system with x coordinate in the direction of flow (along the cavity length), y in the direction normal to the flow (along the cavity width), and z in the direction transverse to the x-y plane (along the cavity height); u, v, and w are the corresponding velocities. The governing equations used are the continuity, momentum and energy equations [7].

The flow is considered to be incompressible, viscous and Newtonian. The steady-state conservation equations governing the transport of mass, momentum and energy are expressed as follows:

Continuity equation (Equation 3.1):

$$\frac{\partial u}{\partial x}+\frac{\partial v}{\partial y}+\frac{\partial w}{\partial z}=0 \tag{3.1}$$

In particular the mathematical model of Flow 3D® is according to the equation (Equation 3.2):

$$\frac{\partial C}{\partial t}+u\frac{\partial C}{\partial x}+v\frac{\partial C}{\partial y}+w\frac{\partial C}{\partial z}=\frac{1}{V_f}\frac{\partial C}{\partial t}+uA_x\frac{\partial C}{\partial x}+vA_y\frac{\partial C}{\partial y}+wA_z\frac{\partial C}{\partial z} \tag{3.2}$$

This equation is integrated with the geometrical model into the computational mesh. Where $V_f$is the volume fraction relative to a cell of the mesh and A_x, A_y and A_z are the area vectors [31].

Momentum balance equations (Navier-stokes equation) are represented like (Equation 3.5):

$$\rho\left(u\frac{\partial u}{\partial x}+v\frac{\partial u}{\partial y}+w\frac{\partial u}{\partial z}\right)=\mu\left(\frac{\partial^2 u}{\partial x^2}+v\frac{\partial^2 u}{\partial y^2}+w\frac{\partial^2 u}{\partial z^2}\right)-\frac{\partial p}{\partial x} \tag{3.3}$$

The equation solved for x. It is solved for y and z using the same method. After applying these equations to the particular mathematical model of Flow 3D®, the equations are expressed as follow (Equation 3.4):

$$\frac{\partial u}{\partial t}+\left(u\frac{\partial u}{\partial x}+v\frac{\partial u}{\partial y}+w\frac{\partial u}{\partial z}\right)=-\frac{1}{\rho}\frac{\partial p}{\partial x}+g_x-\frac{1}{\rho}\Delta\tau_x-Ku-\frac{RSOR}{\rho}u-F_x \tag{3.4}$$

As in the before equation, this is solved for x. It is divided in terms where $U = (u, v, w)$ is the fluid velocity, p is pressure; g gravity and non-inertial body acceleration; τ is the viscous stress tensor; Ku is drag (porous baffles, obstacles, mushy zone); $RSOR(u/\rho)$ are accelerations caused by mass injection at zero velocity; F is other forces as surface tension, electric forces, mass/momentum sources, particles, user-defined forces [6,30].

Heat transfer equation (Equation 3.5):

$$\rho C_p\left(\frac{\partial T}{\partial t}+u\frac{\partial T}{\partial x}+v\frac{\partial T}{\partial y}+w\frac{\partial T}{\partial z}\right)=\lambda\left(\frac{\partial^2 T}{\partial x^2}+\frac{\partial^2 T}{\partial y^2}+\frac{\partial^2 T}{\partial z^2}\right)+L\frac{\partial f_s}{\partial t} \tag{3.5}$$

Where ρ is density; t the time;p the pressure; C_p the specific heat of molten metal; λ the thermal conductivity; T the temperature; L the latent heat and f_s the solid phase fraction at the solidification stage [13].

3.3 Control Volume Approach

This topic is based on the structured finite difference grid. The grid is staggered so that scalar quantities are stored in cell centers while vector and tensors quantities are stored in the cell faces (Figure 3.1).

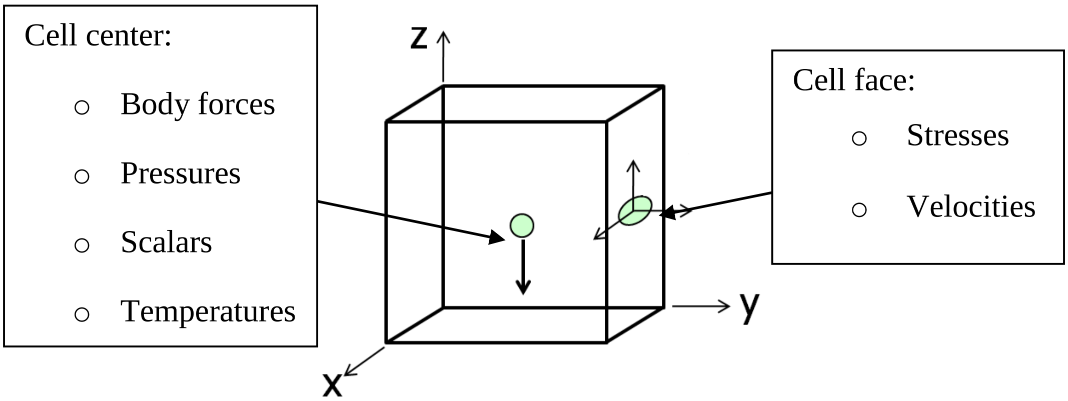

Figure 3.1 - Cell representation of scalar and vector quantities [31]

The solution of the Flow 3D® is performed on a mesh of staggered finite differences. The mesh is staggered so that scalar quantities, such as temperature and pressure, are calculated in cell centers and the vectors and tensor are computed on the faces of the cells. This approach provides a very stable and convenient way to derivative computation [29].

The limits are represented accurately using a technique of Fractional Area Volume Obstacle Representation (FAVOR®).

FAVOR® is a technique for the representation of complex geometry in a structured grid using cells fractional volumes and areas [31,32]. When geometry is imported into Flow 3D®, the first step of action is the preprocessor implementation of the geometry in the computational grid. The reckoning of the geometry is made by computing which cells are blocked, open and fractionally blocked. The volume of a cell that is open is represented by Volume Fullness (VF), which is 1.0 to fully open cells, and the same happens with Area Fullness (AF). The practical case can be seen in Figure 3.2, where the definition of the geometry of the volume and area ratios of the cells represented in equations 3.6 and 3.7 is needed [31].

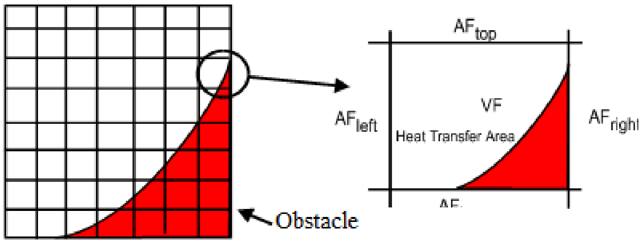

Figure 3.2 - Fractional area representation [31]

$$VF = \frac{Open\ Volume}{Volume\ of\ Cell} \tag{3.6}$$

$$AF = \frac{Open\ Area}{Cell\ Edge\ Area} \tag{3.7}$$

There are 5 measurable quantities that are needed to characterize a geometry, which are:

- Fraction of the area of the face of the cell (3);
- Cell volume fraction;
- Heat transfer area.

This technique is achieved through the integral conservation Equations 3.8:

$$\frac{\partial C}{\partial t} + u\frac{\partial C}{\partial x} + v\frac{\partial C}{\partial y} + w\frac{\partial C}{\partial z} \rightarrow \frac{1}{V_f}\frac{\partial C}{\partial t} + uA_x\frac{\partial C}{\partial x} + vA_y\frac{\partial C}{\partial y} + wA_z\frac{\partial C}{\partial z} \tag{3.8}$$

The FAVOR® advantages, over the body fitted grid, is that the gridding is greatly facilitated because the preprocessor does all the work and changes can be made to the geometry without changing the mesh in most cases. The staggered grids have some disadvantages when using single mesh blocks. For example, when a twisting flow domain is modeled, the fine resolution used in the channel extends beyond the channel, wasting simulation memory [32].

Moreover, when modeling the flow over an object, the grid may have to be well resolved, close to the object to capture thermal and viscous boundary layers. This makes the resolution of the near-object to extend into regions where this resolution is not necessary or desired (Figure 3.3).

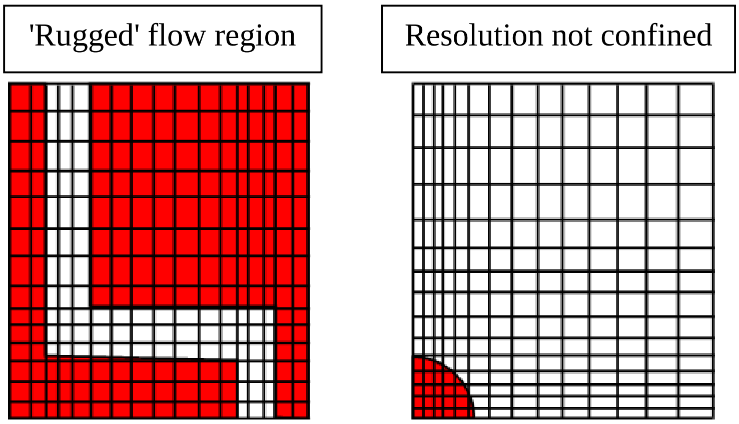

Figure 3.3 - Example of cases where a single mesh block is not efficient [31]

The solution to this problem is multiple mesh blocks. There are two types of approaches to the use of multiple blocks available on Flow 3D®. They are linked blocks and nested blocks. Blocks are linked to other blocks connected only at their boundaries and they cannot overlap [31,32]. There aren't special demands on the resolution of the mesh between the blocks in terms of cell sizes or corresponding cells, but the smaller the difference, the better.

This method allows to only outline regions of interest, "saving" simulation memory. This method can be seen in use in Figure 3.4(a). Nested blocks are embedded within another block. The edges may coincide with the edges of the containing block. However, a nested block can't overlap two blocks. Like the linked block, in nested blocks there are no specific limitations on the change in cell size between a nested block and the containing block but, the smaller the change, the better. Thus it is possible to improve the resolution of the geometry in question as observed in Figure 3.4(b) [31,32].

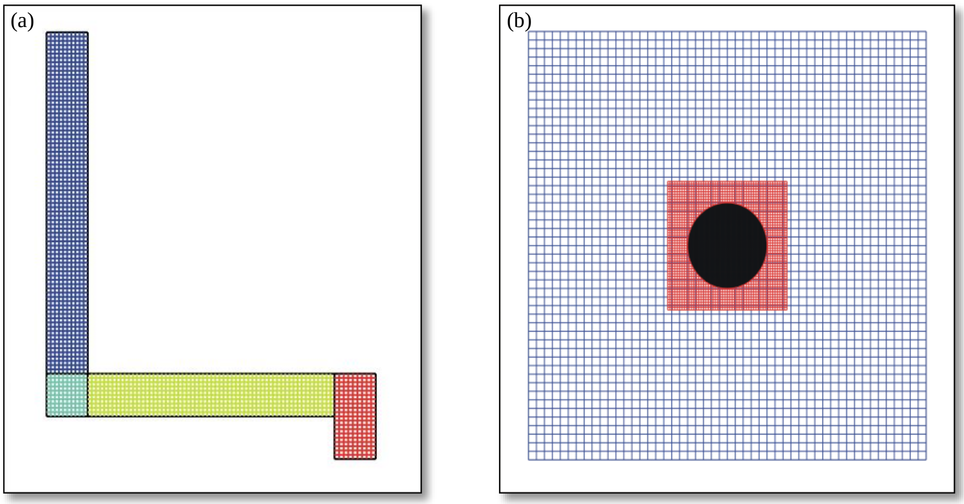

Figure 3.4 - (a) Example of linked blocks, (b) Example of nested blocks [31]

3.4 Volume-of-Fluid Method

This method comes in symbiosis with modeling concepts of free surfaces, namely a liquid/gas interface, having small pressure gradients for the gas and large density ratio between fluids (Figure 3.5) [31,32]. This leads to a modeling approach that only applies the boundary conditions at the interfaces, doesn’t have shear stress at the interface and doesn’t solve governing equations in gas, thus there is nothing to compute. The boundary conditions will be a topic discussed more extensively in Section 3.7. It reflects then on the non-computing of the empty cells thereby reducing the processing capacity [31].

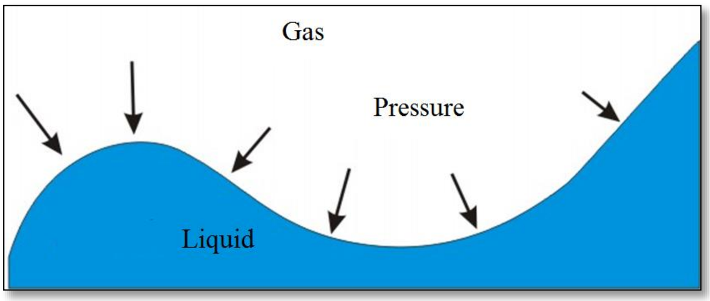

Figure 3.5 - Interaction between fluids [31]

- The volume of fluid (VOF) method provides a more accurate way of advection fluid interfaces via a computer grid, conserving a sharp and well defined interface. There are three key elements that must be clearly defined in any CFD tool, to be labelled a VOF method. Firstly, there must be a fluid fraction variable F, which controls the amount of fluid within a given computational cell. Secondly, one advection algorithm is necessary not only to set F, but to maintain the sharp interface (Figure 3.6) [31].

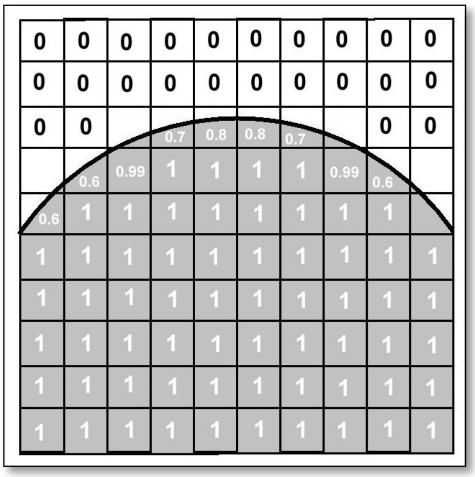

Figure 3.6 - Representation of the VOF method [7]

Thirdly, the free surface boundary conditions should be applied to the interface. The free surface boundary conditions are: being under normal pressure and without shear stress.

The three components of the VOF method are [31]:

- F = Fluid fraction (which is equal to 1.0 in fluid regions, and equal to 0.0 in voids), averaged over a computational control volume, the fluid fraction function has a fractional value in cells containing a free surface;
- A special advection algorithm is used for tracking sharp free surfaces;
- Zero shear stress and constant pressure boundary conditions.

As mentioned before, any numerical technique that claims to be labelled a VOF method should include an algorithm for advection interface and keeping it sharp. It should be noted that the advection is the diffusion process of any form of energy or mass within a fluid. The advection scheme in this software is called TruVOF® since it satisfies these requirements and includes improvements to maintain the sharp interface. The TruVOF® technique contains a logical platform that determines how the fluid is guided within a surface cell so that it is in accurate advection to neighboring cells. For example, if the fluid fraction is 0.5 (half cell), the orientation of the fluid must be determined based on the fluid fraction of the neighboring cells [7,32].

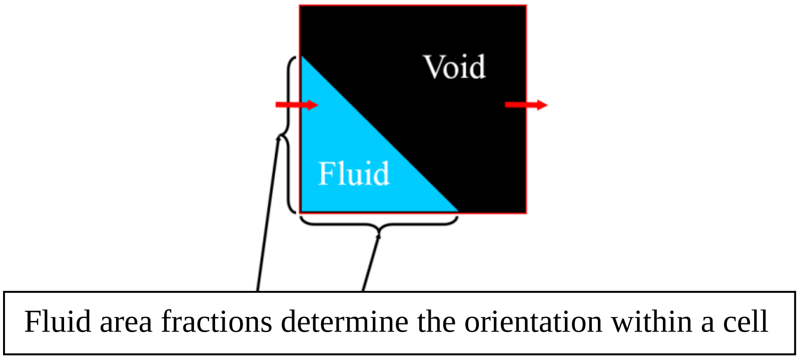
Void
Fluid
Fluid area fractions determine the orientation within a cell

Figure 3.7 - TruVOF representation [31]

The other VOF methods of another commercial CFD codes do not use these three elements but use a variable density method with high-order advection schemes to try to minimize the spread [31].

3.5 Construction of the Geometric Model

The geometric models in Flow 3D® are named by components and, consequent, subcomponents. A geometry consists of one or more components that are then divided into subcomponents. A subcomponent is an object that defines a particular geometry, such as a cylinder, sphere or more complex 3D geometry. Each component has uniform material and movement properties. Objects defined as sub-components specified in a component have the same material properties, such as density, thermal conductivity, surface roughness, etc. If a component is defined as a component "movement" all its sub-components (objects) will move as a single entity. Various definition and creation methods of a component are used by setting various forms for solids (for example, sphere, cylinder or rectangular block); through CAD data from various types of files: stereolithography *(STL)*, *IDEAS*, tetrahedrons data or ANSYS; or topographical data, which is a file of x, y, z coordinates [33].

A component can be set as the standard, porous, lost foam, domain removing or core gas. There are other designations however the most frequently used. Subcomponents can be defined as a solid, hole or complement [34].

A standard component is the most commonly used option. This characterization was used in the simulation. It implies that the defined geometry is a solid object. Most objects that use this kind of geometry will be the die, shot sleeve, piston and ladle for casting simulation, spillway, river bottom, pipes and channels for hydraulics simulation, micro-nozzles and micro channels for microfluidics simulation [32,33].

A porous component implies that all the subcomponents grouped under the same component are as porous as a filter. The filter characteristics are defined by specifying porous properties: porosity and drag coefficients. If a cylindrical filter is required within a tube is not necessary to model the filter with the pores in it, is modeled only within a cylinder tube and is subsequently defined as porous [32,33].

Lost foam is a special type of component that characterizes the foam loss in this process. This type of material volatilizes with the proximity of liquid metal.

Domain removing is fit for the user to disable a specific part of the mesh. This characterization is used when there are large open areas of computational domain known to remain void of fluid throughout the simulation. Not applying this characterization would require the use of a greater amount of memory and increase unnecessary need for more computational power [32,33].

Core gas allows to define a gas barrier core with the thermophysical properties of the sand through the chemical properties of the binder and the flow characteristics of the aerated binder. This allows to acquire a flow of gas of chemical binder in permeable molds and cores [32,33].

In the geometry it is possible to create a baffle. A baffle is a porous zero thickness geometry that controls or directs fluid flow. Its geometry can be flat, cylindrical, spherical or conical. They're also used to calculate the fluid flow rates and to count the particles that pass through the baffle [32–34].

3.6 Meshing

The mesh blocks are covering the geometry of the part to incorporate a fluid region. These blocks define the overall length of the flow and mold. The mesh dimensions may be bigger or smaller than the geometry of the piece under study. Mesh blocks can be linked or nested as already outlined in Chapter 3.3. The mesh defines how accurate the delineation of the geometry is, which can be observed immediately using the FAVOR® technique, and it can be set by cartesian or cylindrical coordinates. It is possible to check the progress of the process in Figure 3.8, where initially the geometry is overlapped by the mesh (Figure 3.8(b)), the mesh is later characterized and ultimately the FAVOR® method is used (Figure 3.8(c)) to validate the flow model [35].

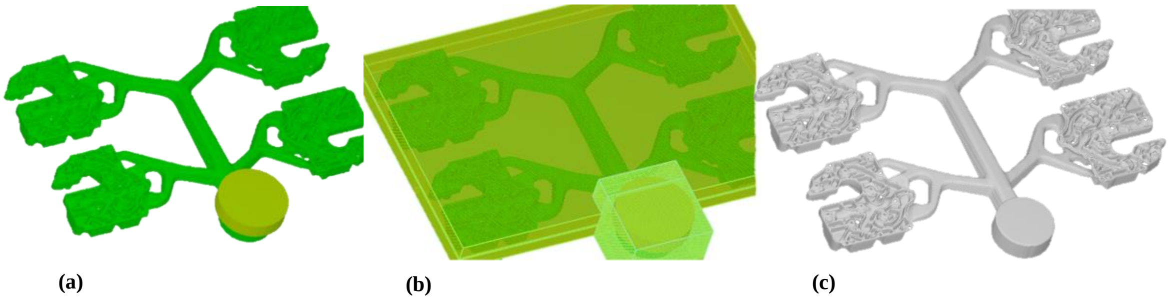

Figure 3.8 - (a) Geometric model, (b) Meshed model, (c)Favorized mode [35]

In cases using linked mesh blocks their frontiers must match properly and have a match of boundary conditions made automatically through the preprocessor. Each block may have a different cell resolution, it is important however, that this difference not to be accentuated where there is a confluence of flows. Taking this into account the errors are prevented on the flow geometry, this is because, the model accuracy is reduced if the cells do not align [32,35].

The technique used for a mesh refinement is, the use of fixed points, smoothing the link between blocks that are not aligned. The presented technique consists of fixating the coordinates which are mutual in the mesh grid, thus obtaining a mesh grid alignment. In the Figure 3.9 the application of the technique of fixed points is exemplified [35].

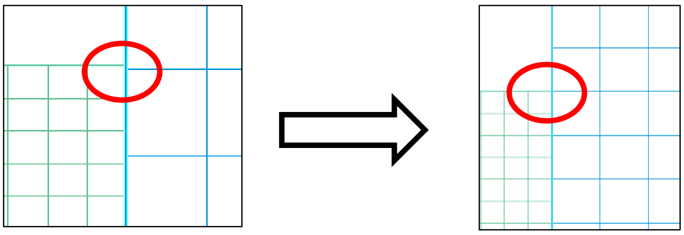

Figure 3.9 - Application of the fixed points [35]

When transferring an object to the discrete mesh, the mesh grid is too rough, thus too many details will be lost. It is noted that the component must occupy at least a grid point of intersection. If this is not done, that information will be lost. Another important feature is that Flow 3D® calculates the cell area blocked by the object and then draws a line in a linear manner throughout the cell. This will cause the edges of the component to be lost and the rounded objects to lose their curvature. In Figure 3.10 examples of this kind of error can be seen [32,35].

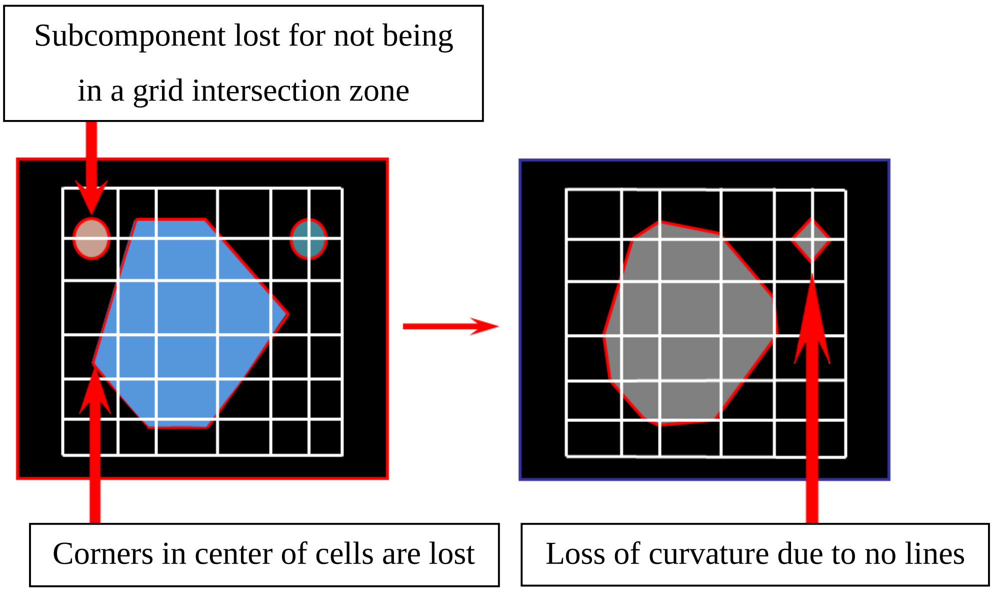

Subcomponent lost for not being in a grid intersection zone

Corners in center of cells are lost

Loss of curvature due to no lines

Figure 3.10 - Errors from rough mash grids [35]

Finally, in order for a fluid to enter the domain of a component, the mesh should be placed slightly below so that there is open volume above the mesh. This way the software recognizes the entry of the fluid in question. In Figure 3.11 that situation is represented [32,35].

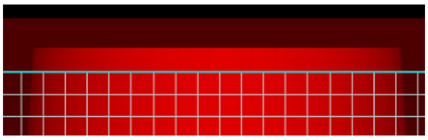

Figure 3.11 - Mesh with open volume

3.7 Boundary Conditions

The boundary conditions can be set for each grid block. In this chapter only the boundary conditions used in the simulation are discussed. For a better study of the different boundary conditions, consider attachment I. The characteristics of different types of boundary conditions used in the simulation will be addressed below.

Symmetric boundary conditions: it is the condition in which there is no mass flow through it. Also no shear stress or heat transfer. This condition is useful to reduce the size of a simulation when there are symmetries in the model and the simulation can be cut at the symmetry plane. In Figure 3.12 the model volume 'cut' to the middle point of symmetry can be observed [32,36]. Since the flow path should be the same around the axis of symmetry, half the model is sufficient. The post-processor can reproduce the missing half of the output such that data can be displayed as a full simulation by turning on symmetry over that axis [32,34,36].

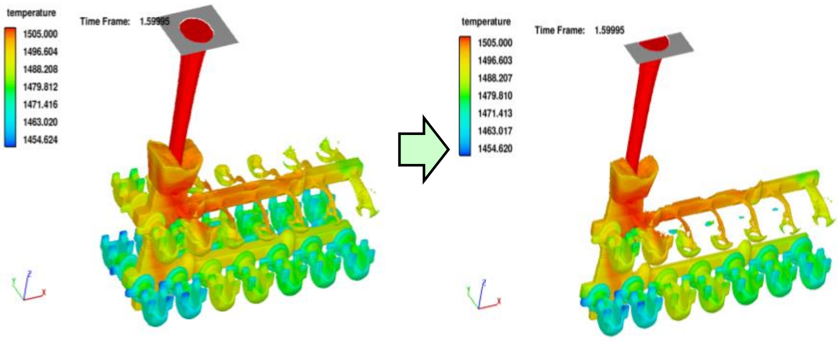
temperature
1505.000
1496.604
1488.208
1479.812
1471.416
1463.020
1454.624
Time Frame: 1.59995
temperature
1505.000
1496.603
1488.207
1479.810
1471.413
1463.017
1454.620
Time Frame: 1.59995

Figure 3.12 - Symmetric boundary [36]

Pressure boundary conditions: The pressure can be constant at the border or time dependent. A time dependent pressure is achieved through a linear interpolation between the set values at each time. When selecting the pressure of stagnation speeds, the velocities upstream are presumed to be zero [32,34,36].

3.8 Physical Models

The Flow 3D® software has a wide range of physical models. In this chapter only the needed models to create a working simulation of low pressure will be addressed.

In some free-surface flows, gas may be entrained at the free surface due to turbulence or the flow conditions. In Flow 3D®, the entrainment of gas can be parameterized using the two-fluid model or, in one-fluid cases, by selecting the air entrainment model (Figure 3.13 (a)). This model estimates the rate at which gas (represented by the void regions) is entrained into the flow using a balance of stabilizing forces (gravity and surface tension) and destabilizing forces (turbulence) [34,37]. The model may be used for both laminar and turbulent cases. When applying the air entrainment model, the entrainment rate coefficient must be defined to be a positive value; the default value of 0.5 is a suitable starting point for most cases. The surface tension coefficient for pure aluminum is 0.914 N/m [38] and for the A356 at 680º is 80.44 N/m [39]. The aluminum alloy used was the A357, which is of the same class, and since it is really close in percentage values an approximation using the value of 0.86 N/m was made.

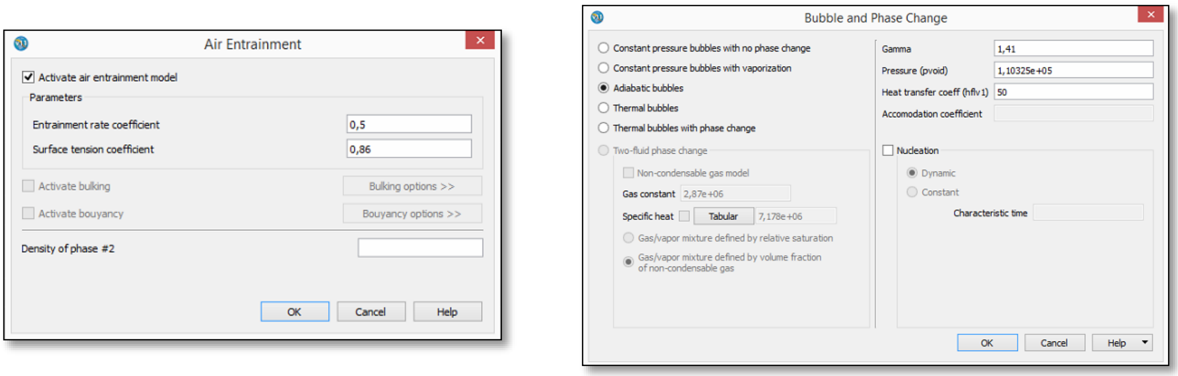
Air Entrainment
Parameters
☐ Activate bulking
Bulking options >>
☐ Activate bouyancy
Bouyancy options >>
OK
Cancel
Help
Bubble and Phase Change
○ Two-fluid phase change
☐ Non-condensable gas model
Tabular
○ Gas/vapor mixture defined by relative saturation
● Gas/vapor mixture defined by volume fraction of non-condensable gas
☐ Nucleation
● Dynamic
○ Constant
Characteristic time
OK
Cancel
Help

(a)

☑ Activate air entrainment model

Entrainment rate coefficient: 0,5

Surface tension coefficient: 0,86

Density of phase #2:

(b)

○ Constant pressure bubbles with no phase change

○ Constant pressure bubbles with vaporization

● Adiabatic bubbles

○ Thermal bubbles

○ Thermal bubbles with phase change

Gas constant: 2,87e+06

Specific heat: 7,178e+06

Gamma: 1,41

Pressure (pvoid): 1,10325e+05

Heat transfer coeff (hflv1): 50

Accomodation coefficient:

Figure 3.13 - (a) Air entrainment parameters, (b) Bubble and phase change parameters

Bubbles must be resolved by a minimum of three cells across the diameter of the bubble, though ten cells is a more practical minimum requirement for an accurate solution [34,37].

The adiabatic bubbles option (Figure 3.13(b)) denotes that the pressure-volume-temperature relationship for the bubble will follow an adiabatic law. In this case, the pressure in each bubble will be inversely proportional to its volume to the power of gamma [34]. As such, it requires that all pressures are specified in absolute terms (rather than gauge values) and that the ratio of specific heats, gamma, is set to a positive number between 1.28 and 1.67.

This bubble models do not apply to bubbles that are in contact with a specified pressure boundary with fluid fraction equal to zero. Those void regions always assume the boundary pressure.

Gravity vector components in a cartesian coordinate system can be simply set in physics, gravity [32,34]. The direction of the gravity vector is constant during a simulation. For this simulation the gravity is set in Z axis being its value -9.81, earth acceleration (Figure 3.14(a)).

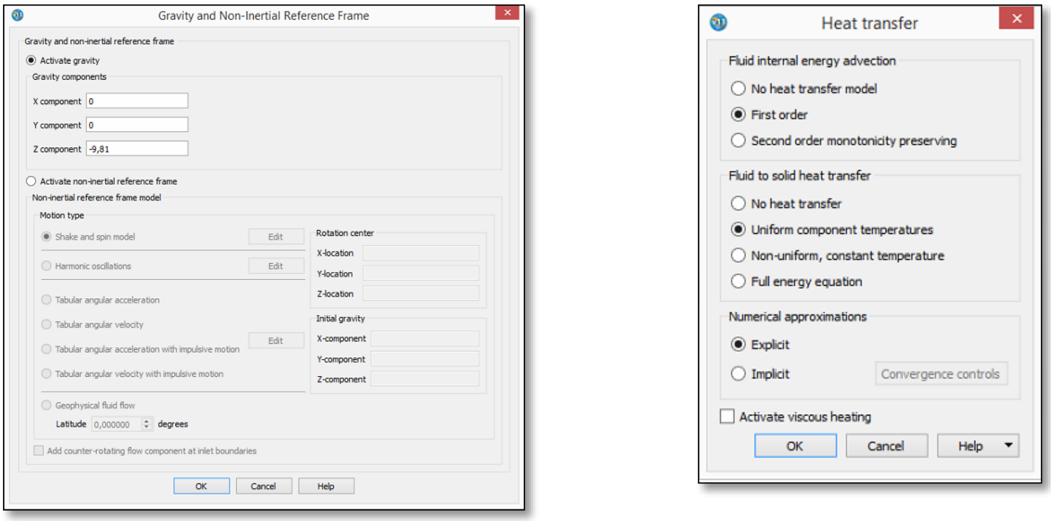

Gravity and Non-Inertial Reference Frame

Gravity and non-inertial reference frame

● Activate gravity

Gravity components

X component: 0
Y component: 0
Z component: -9,81

○ Activate non-inertial reference frame

Non-inertial reference frame model

Motion type

● Shake and spin model
○ Harmonic oscillations
○ Tabular angular acceleration
○ Tabular angular velocity
○ Tabular angular acceleration with impulsive motion
○ Tabular angular velocity with impulsive motion
○ Geophysical fluid flow
Latitude: 0,000000 degrees

Rotation center
X-location
Y-location
Z-location

Initial gravity
X-component
Y-component
Z-component

☐ Add counter-rotating flow component at inlet boundaries

Heat transfer

Fluid internal energy advection
○ No heat transfer model
● First order
○ Second order monotonicity preserving

Fluid to solid heat transfer
○ No heat transfer
● Uniform component temperatures
○ Non-uniform, constant temperature
○ Full energy equation

Numerical approximations
● Explicit
○ Implicit

☐ Activate viscous heating

(a) **(b)**

Figure 3.14 - (a) Gravity and non-inertial reference frame parameters, (b) Heat transfer parameters

For having a uniform heat sources is required that physics, heat transfer, fluid internal energy advection is activated (Figure 3.14(b)).

Uniform component temperatures is activated, where no conduction equation is solved within the components. Each component is treated as a lumped temperature body if solid properties are positive and if the density-specific heat is zero for a specific component (default), the component is treated as having a fixed temperature or a specified surface heat flux [32,34].

The default techniques for advection of momentum and all other fluid quantities are based on explicit numerical approximations. Explicit methods are simple, and relatively accurate, but require limitations in the maximum time-step size. An implicit technique that removes this limitation can be requested in numerics ‣ explicit/implicit solver options ‣ advection. The implicit treatment of the advection terms in the transport equations is applied selectively in cells if it allows the time-step size to be increased without a loss of accuracy [32,34].

The final model used to characterize the fluid was the viscosity and turbulence model (Figure 3.15). In this model it is necessary to select the viscous flow option to characterize the viscosity of the fluid and a laminar regime is wanted.

By far the most common type of boundary conditions are no-slip boundaries, which describe nearly all fluid/solid interfaces

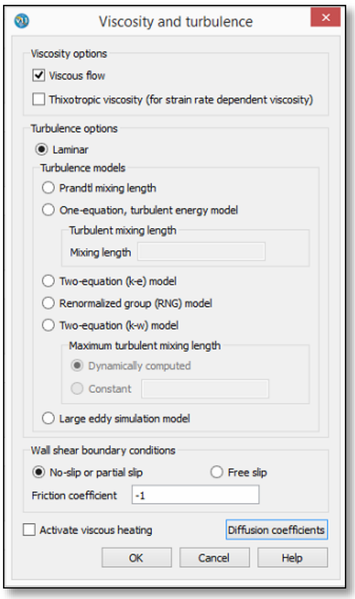
Viscosity and turbulence
Viscosity options
Turbulence options
Turbulence models
Turbulent mixing length
Maximum turbulent mixing length
Wall shear boundary conditions
Diffusion coefficients
OK
Cancel
Help

☑ Viscous flow
☐ Thixotropic viscosity (for strain rate dependent viscosity)
● Laminar
○ Prandtl mixing length
○ One-equation, turbulent energy model
Mixing length
○ Two-equation (k-e) model
○ Renormalized group (RNG) model
○ Two-equation (k-w) model
● Dynamically computed
○ Constant
○ Large eddy simulation model
● No-slip or partial slip
○ Free slip
Friction coefficient -1
☐ Activate viscous heating

Figure 3.15 - Viscosity and turbulance parameters

4. NUMERICAL SIMULATION

4.1 Model Definition (CAD)

In order to evaluate the computational simulation on Flow 3D®, it was necessary to model an assembly of sufficiently complex geometry according to what is planned. To achieve this Inventor® was used, and two pieces were developed, as shown in Figure 4.1 and in Figure 4.3.

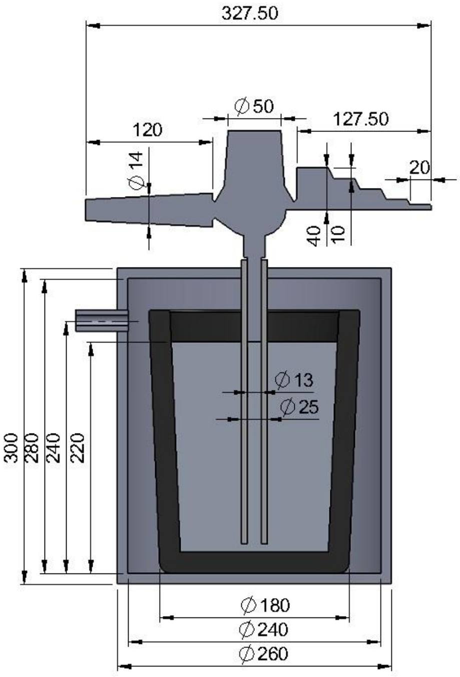

Figure 4.1 - Measurement on Geometric model used in the simulation

The full geometric model was modelled to a system with a reservoir with the air inlet channel, for increasing the pressure. The molten aluminum was placed in a crucible with the rising channel in it to orientate the metal to the final piece. Once it was modeled, it was necessary to import the assembly into Flow 3D® (Figure 4.2(b)). The main difficulty was to assemble the parts correctly because the software does not have a tool to unify the parts. This process is easier if the assembly of the parts, is done on the CAD software first, after that convert the files to STL format and then import to Flow 3D®.

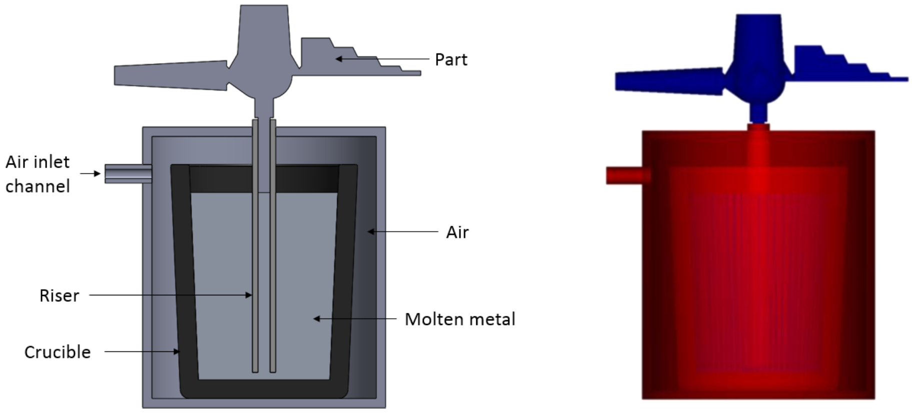
Part
Air inlet channel
Air
Riser
Molten metal
Crucible

(a)

(b)

Figure 4.2 - (a) Geometric model, (c) Flow 3D® model regarding different components (Blue – Hole, Red . Solid)

The second model considered only the casted part. The mold was not modeled because, Flow 3D® it takes into account the characterization of the parts of the models, in which it is possible to add the mold and characterize it in the final piece (without needing to draw it). Note that, for both models, the mold it is expected not to be sealed. The top zone is open in contact with the atmosphere.

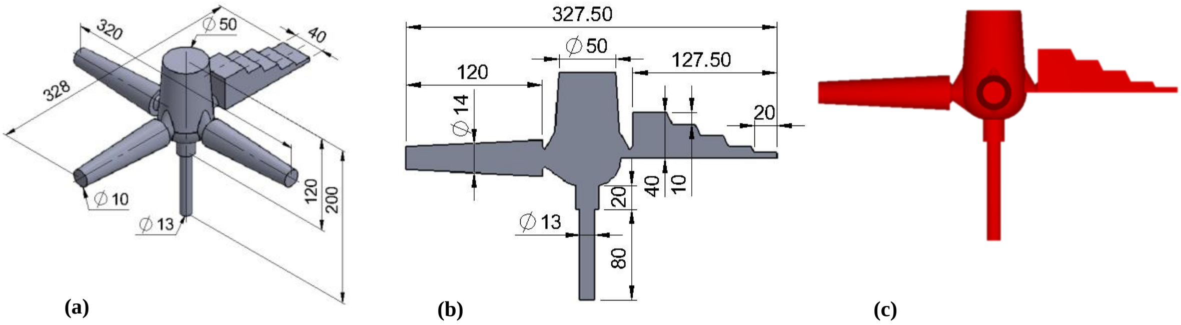
320
⌀50
40
328
⌀10
⌀13
120
200
327.50
⌀50
120
127.50
⌀14
20
⌀13
20
40
10
80

(a)

(b)

(c)

Figure 4.3 - (a) Part for final simulation, (b) section view (c) Flow 3D® model

For the achievement of results, a methodology able to test the geometrical model and the parameters used during the simulation it was needed. This allowed to focus on the origin of the problem, not losing time creating and testing unnecessary models or changing parameter that were correct. For a better understanding a flowchart (Figure 4.4) able to describe the steps made to reach a solution was created:

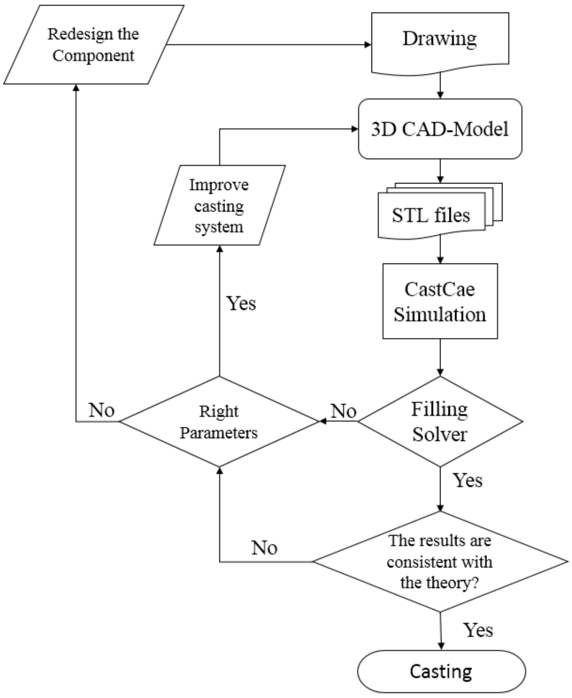
Redesign the Component
Drawing
3D CAD-Model
Improve casting system
STL files
CastCae Simulation
Yes
No
Right Parameters
No
Filling Solver
Yes
No
The results are consistent with the theory?
Yes
Casting

Figure 4.4 - Methodology flowchart

4.2 Numerical Definition

Decide on the geometry to be used it was necessary to define a set of simulation parameters chosen resorting to the existing bibliography and preliminary practical trials in previous works. The used parameters were as follow (table 4.1):

Table 4.1 - Initial conditions of simulation

Conditions	Values
Initial temperature of the fluid	700 ºC
Pressure	Hydrostatic pressure
Initial pressure in the void[1]	$1.01325e^{+5}$ Pa
Temperature in the void	25ºC
Cell size of the mesh	2
Alloy	Aluminum alloy A357
Molding sand	Furan Molding Sand Fine, CB 500 ºC
Gas	Air
Simulation approximately time	15-20s

---

[1] The void in this matter is regarding the environment involving the system. In this case is air.

As described in the previous subchapter the mold was not modeled but only the material Furan Molding Sand Fine, CB 500 ºC was chosen (Figure 4.5). After selecting it, the software has a standard value list according to the chosen material, having the thermal conductivity and density multiplied by the specific heat of die material. This way was possible to calculate the maximum thermal penetration depth through a tool available in the Flow 3D®.

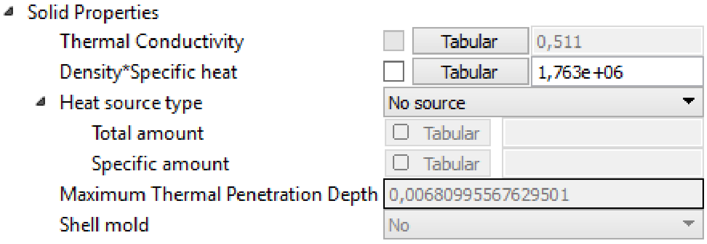

Solid Properties
Thermal Conductivity ☐ Tabular 0,511
Density*Specific heat ☐ Tabular 1,763e+06
Heat source type No source
Total amount ☐ Tabular
Specific amount ☐ Tabular
Maximum Thermal Penetration Depth 0,00680995567629501
Shell mold No

Figure 4.5 - Solid properties from the sand mold

After the choice of parameters it was time to focus on the characterization of the mesh. For the model it was decided to use two mesh blocks. This choice was made to reduce the simulation time by assigning a scarce mesh in the reservoir area because it is not the principal geometry, not being needed so much detail comparing to the final part. The two blocks can't overlap but need to be close enough to make the connection to the physical model. The mesh referring to the casted part was characterized with a more refined mesh to obtain all the details. In the initial phase it was chosen a 7 mm size mesh of the part and 11 mm for the reservoir. To validate this input a tool of the software, called FAVOR®, is used. This tool provides a quick meshing check up to see if the resolution is sharp enough. As it can be seen in Figure 4.6(a) it is visible that the part is not sharp enough. The most noticeable zone is on the right side where it should be a geometry with defined steps but it is like a ramp. The zones with curvature are not well defined too.

The size of the mesh in the reservoir is also too rough as seen in Figure 4.6(b). It is visible that there are missing parts in the reservoir, being able to see holes on the reservoir. It is possible to see that the connection of the molten metal in the riser to the part disappeared. This is because of the error, previously explained, of the two mesh blocks being too far apart.

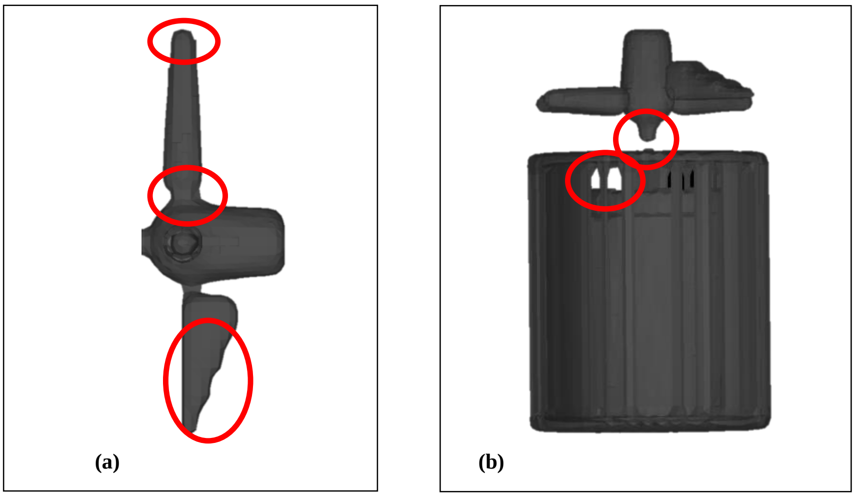

Figure 4.6 - (a)Favorized part with 7mm mesh size, (b) Favorized full model, with 11mm mesh size

To solve this problem, the mesh size was reduced and both meshes were put closer to each other. Regarding the sizes of the mesh, 4 mm was used for the part mesh and 7 mm for the reservoir. After this improvement a better quality of the part is noticeable (Figure 4.7(a)). A sharper geometry, the curved zones were visible and the stair like geometry with a clear defined steps.

The reservoir mesh has also a sharper geometry, being this geometry now complete, not having missing geometry, and the connection between the metal in the rising channel and the part is also clear (Figure 4.7(b)).

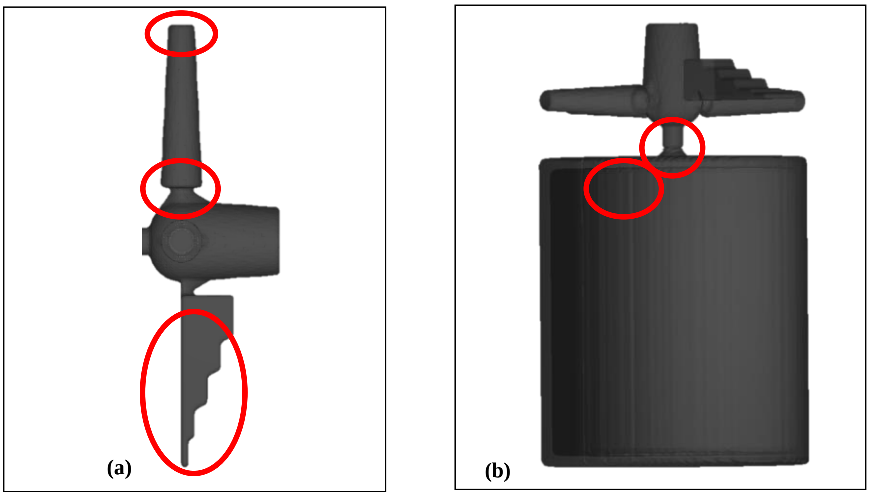

Figure 4.7 - (a) Favorized part with smaller mesh size, (b) Favorized full model with smaller mesh size

Although this was a big improvement to the simulation and having in account the characteristics of the computer used to simulate (Table 4.2), these changes increased, to a considerable amount, the simulation time, because a greater processing speed is needed. The duration of the simulation time with the 11mm and 7mm mesh sizes of 1:30 hours and the simulation with the mesh size of 7mm and 4mm sizes of 8 hours.

Table 4.2 - Computer characteristics used for the simulations

Conditions	Characteristics
Processor	Intel(R) Core(TM) i7-5820K CPU @ 3.50GHz
Memory Size	32 Gbytes 1399.7 MHz
Operative System	Microsoft Windows 8.1 (6.3) Professional 64-bit (Build 9600)

The increasing of time, in a simulation, is a problem because of the need for testing different parameters. Even if something is wrong with the simulation it takes a great amount of time to obtain the results, restraining the amount of simulations. Regarding this problem, and to reduce any possible error originated by the geometries, only the cast part was studied (Figure 4.3). This way only a mesh block and the final part are used, eliminating the probability of errors originated by the full assembly system.

The initial parameters were maintained as the mesh characteristics. Then the best boundary conditions to this model were studied. Being applied air to force the molten metal to rise, the best option for the boundary system was the pressure. The air was applied in the lower zone of the part in the rising channel, so it was set in the z minimum boundary of the mesh block as specified (Figure 4.8).

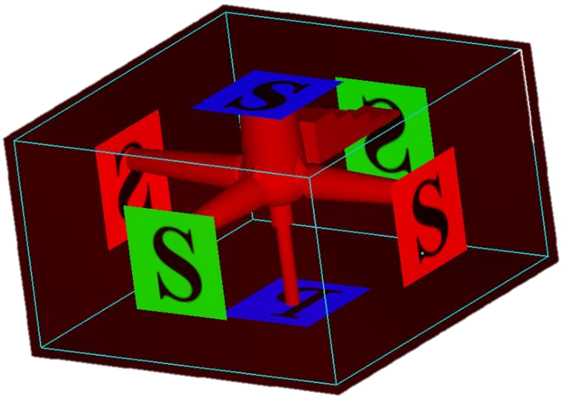

Figure 4.8 – Simulated part with mesh of symmetric boundary conditions and pressure boundary condition in the entry of the molten metal

4.3 Modifications

Throughout this work a range of values for the pressures was used, in order to create the pressure curve (Figure 4.9). For testing, in an initial phase of characterization the pressures were chosen using the support of the bibliography and the iteration method, not being the main focus on the initial phase.

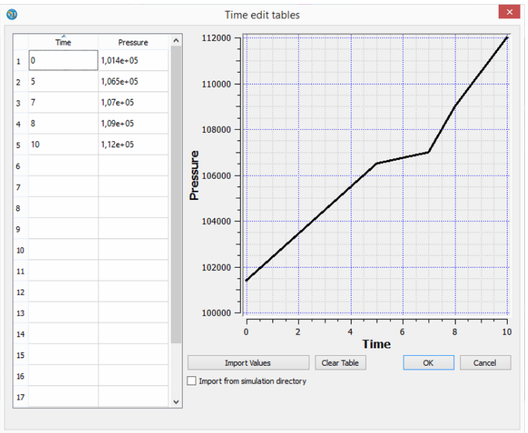
Time edit tables
Pressure
Time
112000
110000
108000
106000
104000
102000
100000
0
2
4
6
8
10
Import Values
Clear Table
OK
Cancel
☐ Import from simulation directory

	Time	Pressure
1	0	1,014e+05
2	5	1,065e+05
3	7	1,07e+05
4	8	1,09e+05
5	10	1,12e+05
6		
7		
8		
9		
10		
11		
12		
13		
14		
15		
16		
17		

Figure 4.9 - Test curve pressure to obtain a fully functional simulation

After running the simulation it was possible to observe that it was running with some error (Figure 4.10) because in the end it was not rising into the channel.

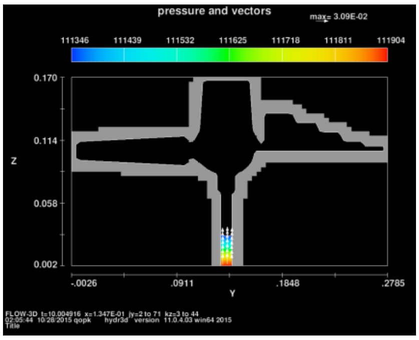

Figure 4.10 – Simulation without the z max open volume

Analyzing the fill fraction graphs, Figure 4.11, it was noticeable that the molten metal only starts to rise after 9s of the simulation. After some consideration, the reached conclusion was that in the simulation the release of air from inside the mold was not happening because it was not considering the open area of z max in contact with the atmosphere.

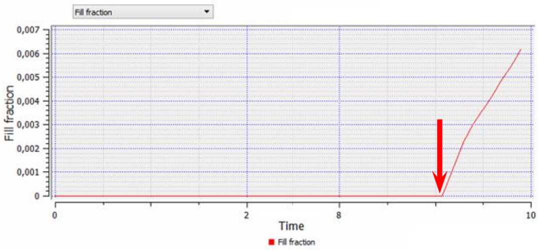

Figure 4.11 - Fill fraction graph of simulation without the z max open volume

As the top area of the part is connected to the atmosphere, it was made the same choice of characterization as in z minimum to the z maximum boundary but in this case the pressure is the same as the atmospheric pressure $1.01325e^{+5}\ Pa$. Both meshes, in this case, are a bit under the geometry (Figure 4.12) as explained in subchapter 3.6.

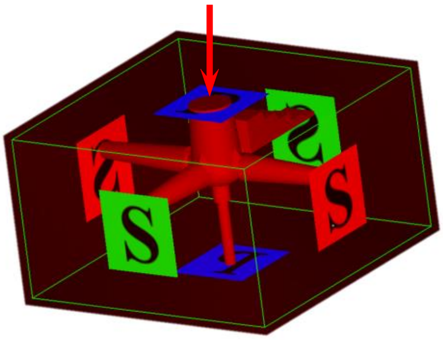

Figure 4.12 - Pressure boundary condition to z maximum open volume

It is clear the improvement of the simulation using the open volume method, having more than 80% of the geometry filled (Figure 4.13).

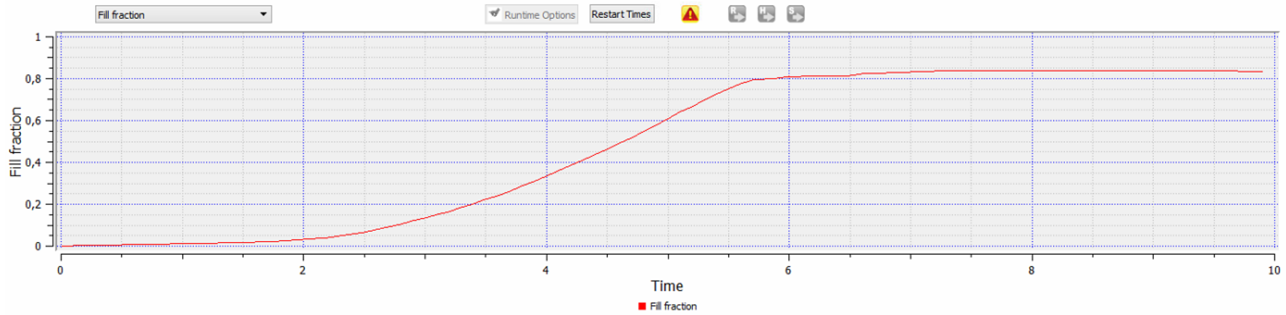

Figure 4.13 - Fill fraction with z maximum open volume

As can be seen in Figure 4.13 the part is almost totally full, being the stair like geometry the problem of the simulation, only filling the first step of the geometry.

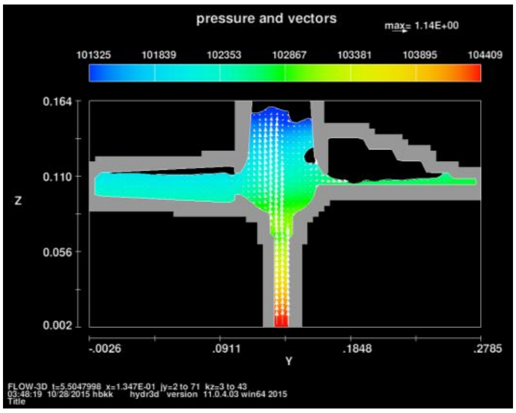

Figure 4.14 - Pressure simulation of z maximum open volume

Analyzing all the simulation it is possible to see that the air was not escaping through the sand mold. This conclusion is made because air bubbles are visible, coming from the stair like geometry, forcing its way out to the center of the part escaping through the hole in the top. To solve this problem a virtual valve was placed in (Figure 4.15), to simulate the permeability capacity, enabling the output of gases to the outside atmosphere.

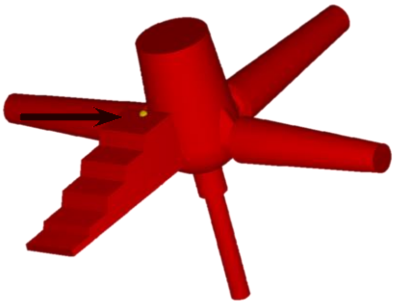

Figure 4.15 - Model with virtual valve to simulate the permeability capacity of the mold enabling the output of gases to the atmosphere

To characterize the valve, parameters shown in Figure 4.16 were used. The valve's external pressure was the atmospheric pressure to simulate the exterior air. The value for the valve loss was used regarding previous preliminary practical tests.

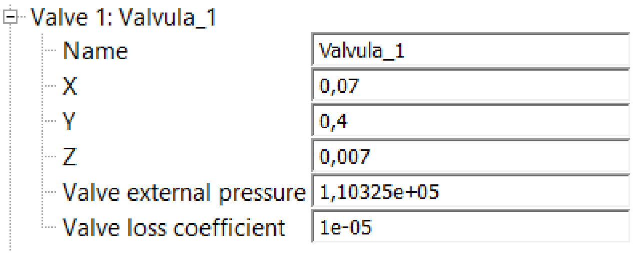

Valve 1: Valvula_1

Name	Valvula_1
X	0,07
Y	0,4
Z	0,007
Valve external pressure	1,10325e+05
Valve loss coefficient	1e-05

Figure 4.16 - Valve parameters used to simulate the permeability of the mold

After placing the valve in the simulation over the geometry, all the geometry was filled with molten metal (Figure 4.17).

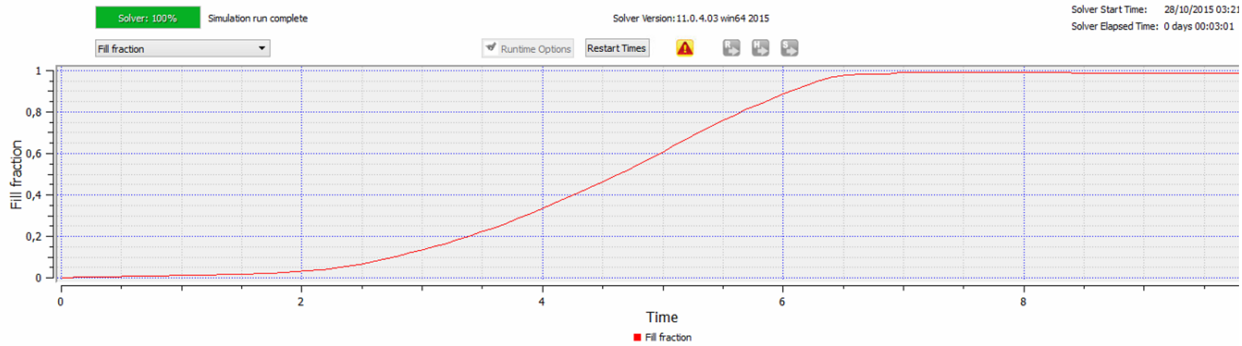

Solver: 100%
Simulation run complete
Solver Version: 11.0.4.03 win64 2015
Solver Start Time: 28/10/2015 03:21
Solver Elapsed Time: 0 days 00:03:01

Figure 4.17 - Fill fraction graph with model with virtual valve

As seen in the simulation the part is full and the pressures make sense, and one can see the greatest value is registered in the rising channel and the lowest value in the open top zone

(Figure 4.18). It is important to highlight the air bubble in the top of the model as being normal, justified by the openness of the mold in that zone, which is not a problem.

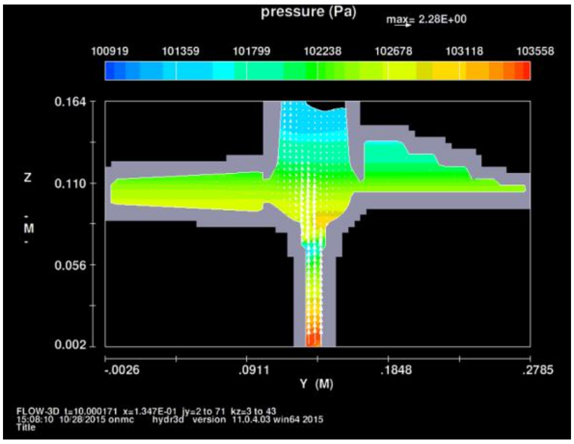

```
FLOW-3D t=10.000171 x=1.347E-01 jy=2 to 71 kz=3 to 43
15:08:10 10/28/2015 onmc     hydr3d  version 11.0.4.03 win64 2015
Title
```

Figure 4.18 - Simulation with virtual valve to simulate the permeability of the mold

After this, the size of the mesh was reduced from 4mm to 2mm to achieve better results by having a more realistic model, not losing information because of the size of the mesh. This modification resulted in an incomplete filling of the part, Figure 4.19

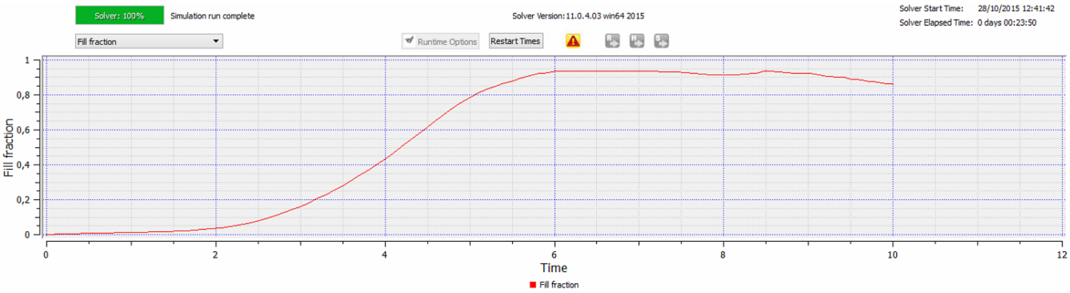

Solver: 100% Simulation run complete

Solver Version: 11.0.4.03 win64 2015

Solver Start Time: 28/10/2015 12:41:42
Solver Elapsed Time: 0 days 00:23:50

Figure 4.19 - Fill fraction graph with 2mm mesh size

Examining the simulation it is possible to see that the conic geometries didn’t fill, just like in the same situation explained before considering the stair like geometry (Figure 4.20).

This was because of the refinement of the mesh being able to obtain more details that compromised the air escape, considering that setting the 4mm mesh size causes the grid not to intersect all the geometries, leading to mesh errors which were discussed in section 3.6.

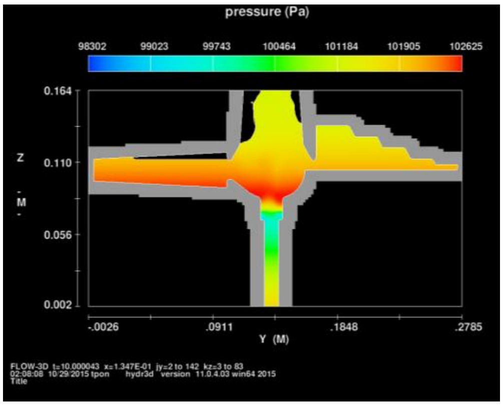

```
FLOW-3D t=10.000043 x=1.347E-01 jy=2 to 142 kz=3 to 83
02:08:08 10/29/2015 tpon     hydr3d  version 11.0.4.03 win64 2015
Title
```

Figure 4.20 - Simulation with 2mm mesh size

Using the FAVOR® tool, it is possible to look how much of a difference from the 4mm mesh size was to the 2mm. With the loss of the geometry, regarding the 4mm mesh size (Figure 4.21(a)), in the entry channel, this zone seems more open, being able for the air to escape more easily. Lowering the size of the mesh for 2 mm (figure 4.21(b)), allows to intersect more points of geometry, being more realistic, narrowing the entry of the molten metal, entrapping the air.

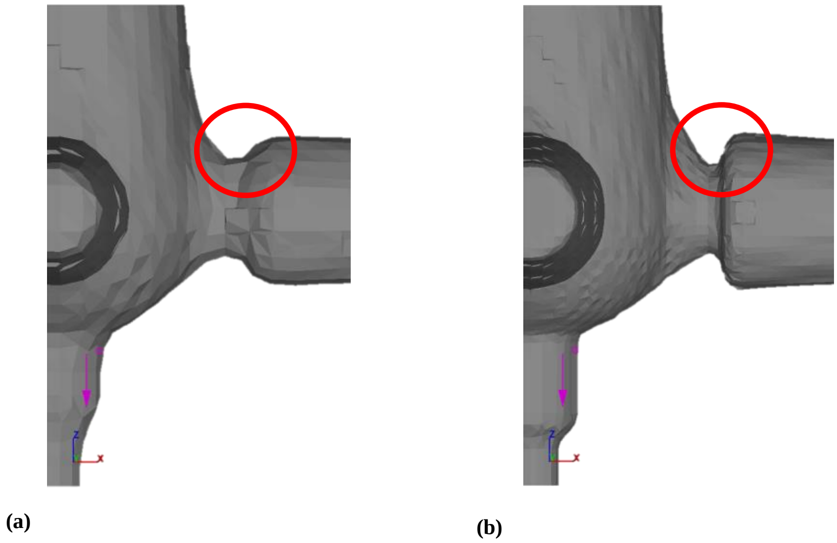

(a) **(b)**

Figure 4.21 - (a) Favorized part with 4mm mesh size, (b) Favorized part with 2 mm mesh size

The approach to the solution for the problem was the same as with the stair like geometry, putting valves for the same reason (Figure 4.22).

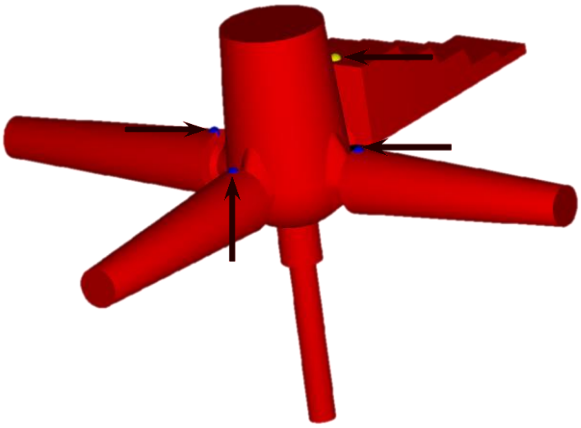

Figure 4.22 - Model with virtual valves to simulate the permeability of the mold regarding the entry zones of molten metal

As visible on the simulation, the solution worked, not having any blocked air in any part of the model, being completely full (Figure 4.23).

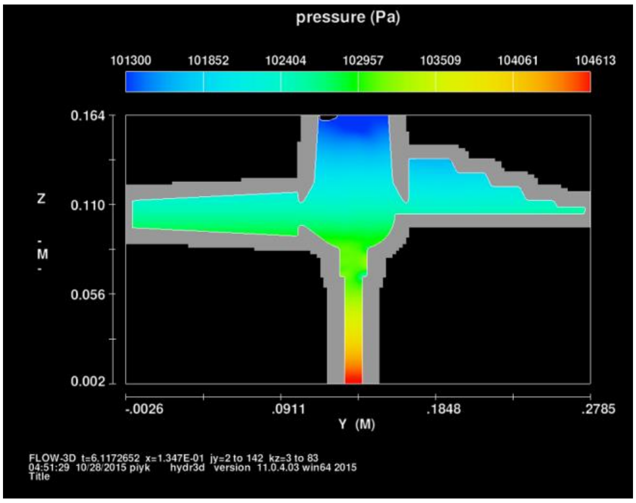

Figure 4.23 - Simulation with valves

Although the simulation was working, when analyzing the center of the part it was visible that still some air was being pushed to the center, originating a swirl of the fluid in the center. This problem's origin was the air located in the extremities of the parts pressuring to the molten metal entering. This pressure, originated with the escaping air, was creating a wave of fluid, being the cause of the problem. To solve this, valves were also put in the extremities of the parts (Figure 4.24).

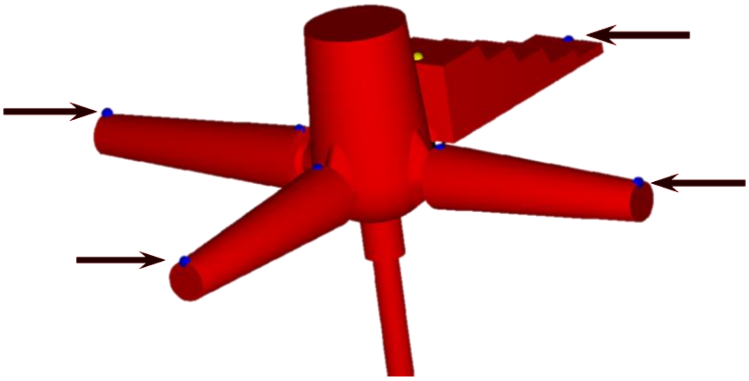

Figure 4.24 - Model with virtual valves in the extremities of the geometries to simulate the permeability of the mold promoting a more uniformed filling

With a fully operational simulation it was time to focus on the pressure curves. The chosen values for the curves were made regarding preliminary practical tests from previous works.

4.4 Final Simulations

Having a fully functional simulation the only parameters changed were the initial conditions and the pressure curve (Table 4.3). All the other variables in the system are maintained constant.

Table 4.3 - Tested pressure curves

Pressure curve	M1 (0 – 5 s)	M2 (5 – 10 s)	M3 (10 – 15 s)	M4 (15– … s)	Observation
Pressure curve 1	1400 Pa/s	400 Pa/s	0	0	Curve with 2 ramps
Pressure curve 2	600 Pa/s	400 Pa/s	800 Pa/s	0	Curve with 3 ramps

For the pressure curve 1the used initial parameters were (table 4.4):

Table 4.4 - Initial conditons of simulation of pressure curve 1

Conditions	**Values**
Initial temperature of the fluid	700ºC
Pressure	Hydrostatic pressure
Initial pressure in the void	$1.01325e^{+5}$ Pa
Temperature in the void	25ºC
Cell size of the mesh	2.5
Alloy	Aluminum alloy A357
Molding sand	Furan Molding Sand Fine, CB 500 C
Gas	Air
Simulation (approx.) time	20s

The pressure curve for the simulation has 3 stages of pressure and it is as follows (Figure 4.25):

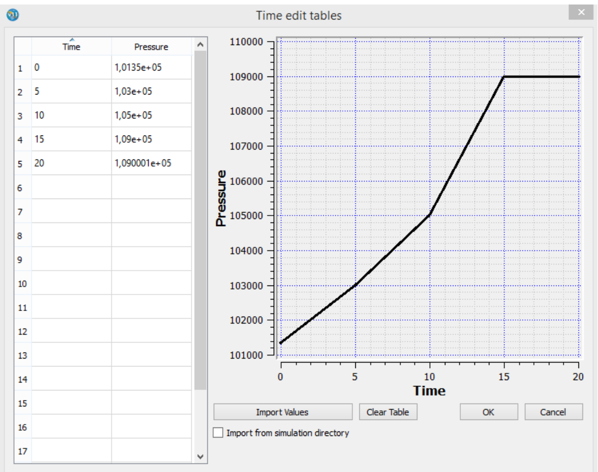

	Time	Pressure
1	0	1,0135e+05
2	5	1,03e+05
3	10	1,05e+05
4	15	1,09e+05
5	20	1,090001e+05
6		
7		
8		
9		
10		
11		
12		
13		
14		
15		
16		
17		

☐ Import from simulation directory

Time edit tables
Pressure
110000
109000
108000
107000
106000
105000
104000
103000
102000
101000
0
5
10
15
20
Time
Import Values
Clear Table
OK
Cancel

Figure 4.25 - Pressure curve 1

At the end of the simulation, the fill fraction graph (Figure 4.26) shows that the time to fill the entire model was approximately 12s.

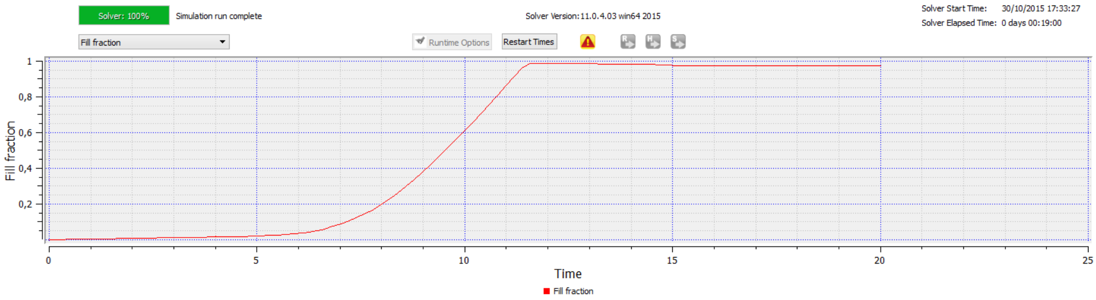

Solver: 100% Simulation run complete

Solver Version: 11.0.4.03 win64 2015

Solver Start Time: 30/10/2015 17:33:27

Solver Elapsed Time: 0 days 00:19:00

Fill fraction

Figure 4.26 - Fill fraction pressure curve 1

Analyzing the simulation of the behavior of the pressure in the part (Figure 4.27), at approximately 9s the highest pressure occurs at z min, $1.03664e^{+5}Pa$ and the lowest pressure is in the fluid in contact with the atmosphere, $1.01321e^{+5}Pa$ (Figure 4.27(a)). This happens because it is the rising channel, so, it is the zone where the pressure is being made, so that the molten metal rises. It is lower at the molten metal that is in contact with air because only the atmospheric pressure is actuating. Against this, at 10s (Figure 4.27(b)), the molten metal at the top, as it goes into contact with the mold, raises the pressure to $1.03918e^{+5}Pa$.

It lowers through time, but maintains a certain pressure value due to the molten metal being in contact with the mold and the force made by the rising metal. In the middle of the part and at the end of the simulation (at 20s), the pressure registered has a value of $1{,}02635e^{+5}Pa$ (Figure 4.27(d)). Pressures are lowering gradually, from z max to z min being the highest pressure is $1.03963e^{+5}Pa$, located in the z min zone. The lowest pressure is $1.01307e^{+5}Pa$, at the top of the part. This pressure, in the z max, is a normal consequence because it is the zone connected to the atmosphere.

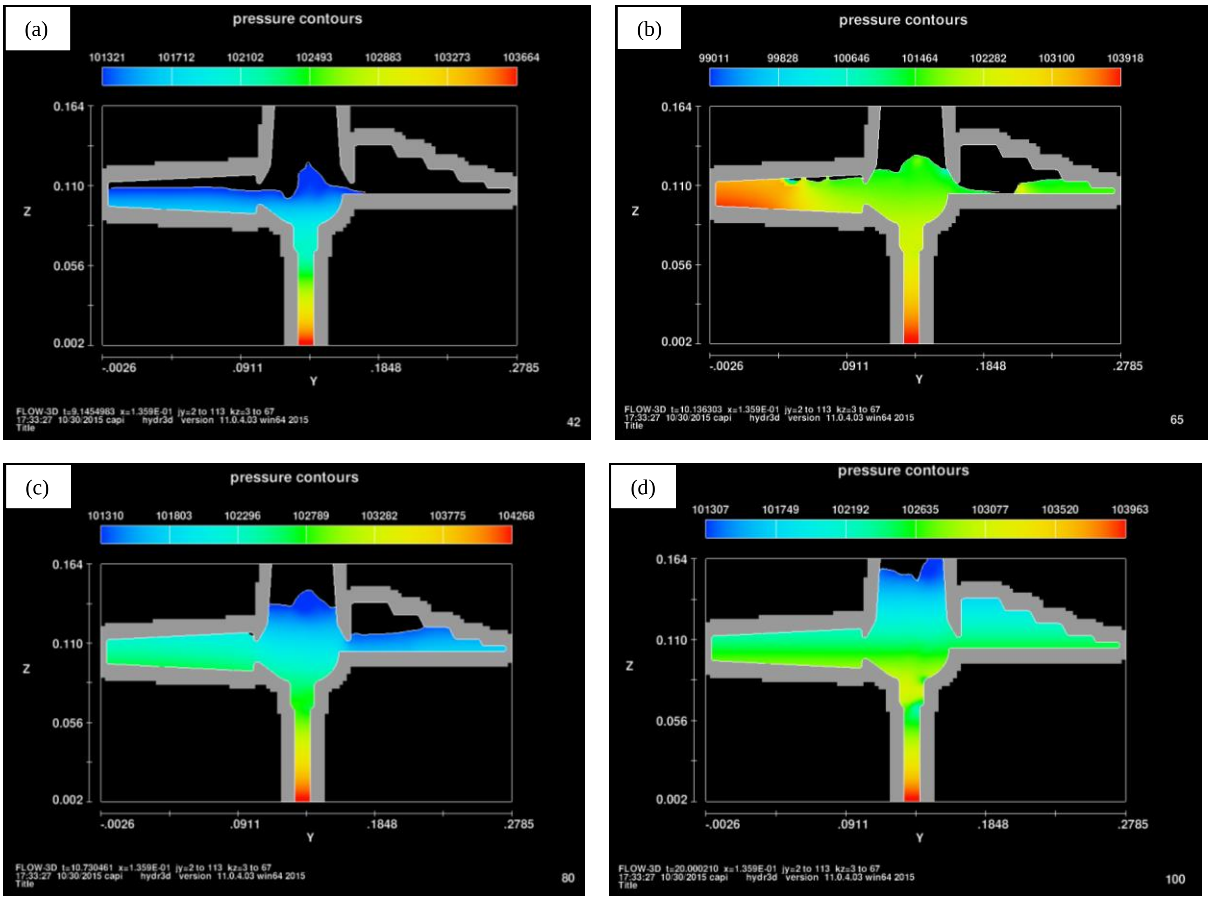

Figure 4.27 – Values of pressure contours for simulation of p-t (1): (a) values at 9.15s, (b) values at 10.14s, (c) values at 10.73s, (d) values at 20s

Studying the temperature simulation (Figure 4.28), it is perceptible that the temperatures are lowering at the extremities during the entire simulation. A normal behavior, since these parts are thinner, suffering more dissipation of heat. The rising channel is the zone with the highest temperature, because the molten metal rises from the crucible through the channel, being initially at 700ºC. The center part, because of its thickness and being the immediate zone to constantly receive new metal, is also one of the hottest zones, losing temperature airwards and reaching a temperature of 650ºC (Figure 4.28(d)). The cone geometry part is one of the zones that has the most heat dissipation, being the temperature around the 420ºC in the entrance of the metal and about 280ºC throughout the rest of the geometry. The stair like geometry is an interesting case, being thicker in the entrance of the metal, which leads to temperatures around 460ºC. The extremity of this zone is the one with the lowest temperature, because of it being thin, having temperatures around 214ºC.

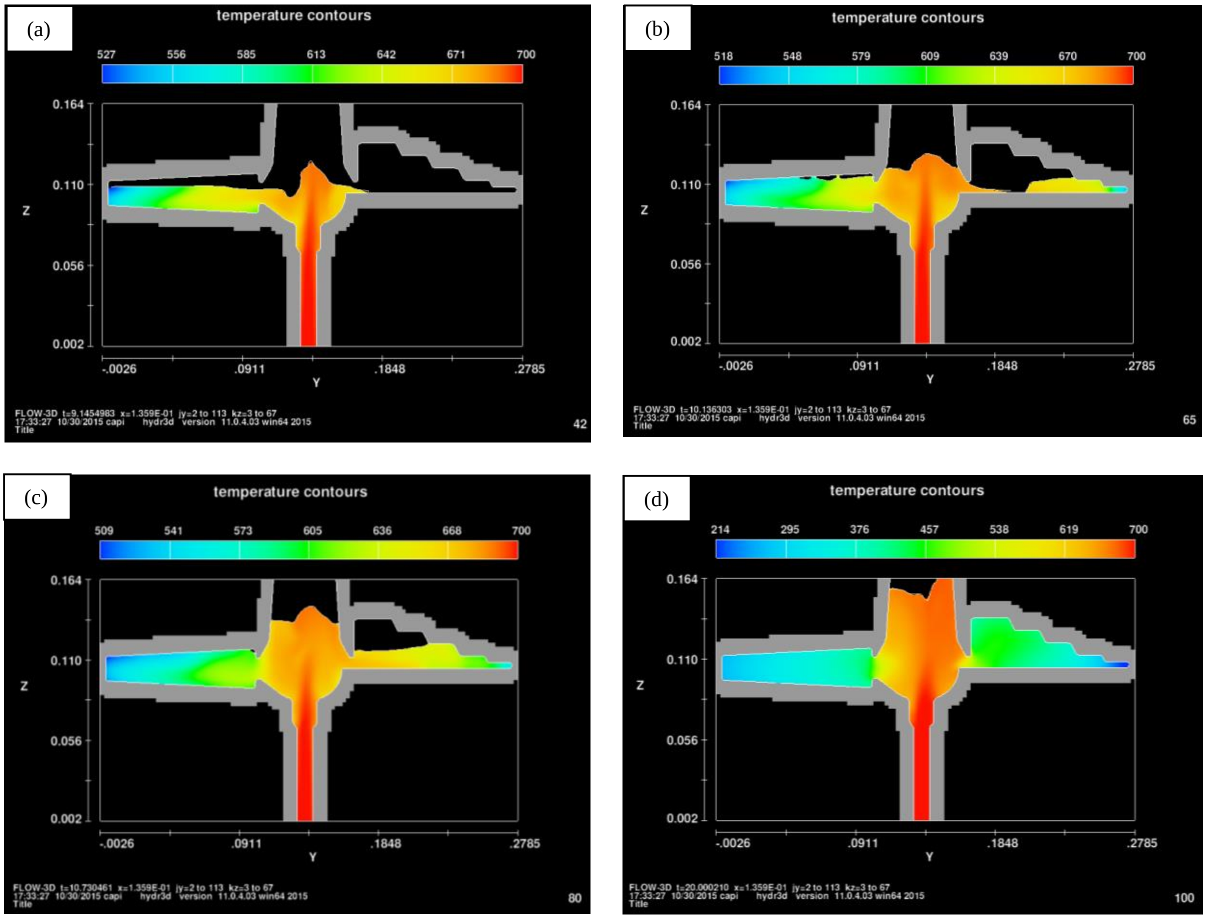

Figure 4.28 – Values of temperature contours using the uniform component temperatures heat transfer parameter for simulation of p-t: (a) values at 9.15s, (b) values at 10.14s, (c) values at 10.73s, (d) values at 20s

In the simulation of the velocities (Figure 4.29), at approximately 9s (Figure 4.29(a)) the highest velocity is in the rising channel, because of the amount of molten metal pushed into the part. This velocity rises to $1\,m/s$ through time, not being problematic because it doesn’t affect the part. Over all, in the simulation, the velocity reached in the center of the part is around $0.35\,m/s$. This validates the simulation because, if the velocity was higher then $0.5\,m/s$, this meant it was a turbulent regime. Being turbulent, entrainment of the oxide films occurs which causes major damage to the castings [15]. The velocity in the entrance of the stair like geometry is around $0.45\,m/s$, due to the narrowness of the entrance, creating more pressure to the flux entry. The velocity in the cone part is $0\,m/s$ since the part is totally full (Figure 4.29(c)). The velocity in the end of the simulation (Figure 4.29(d)), in the cone and the stair like geometry is $0\,m/s$, being full.

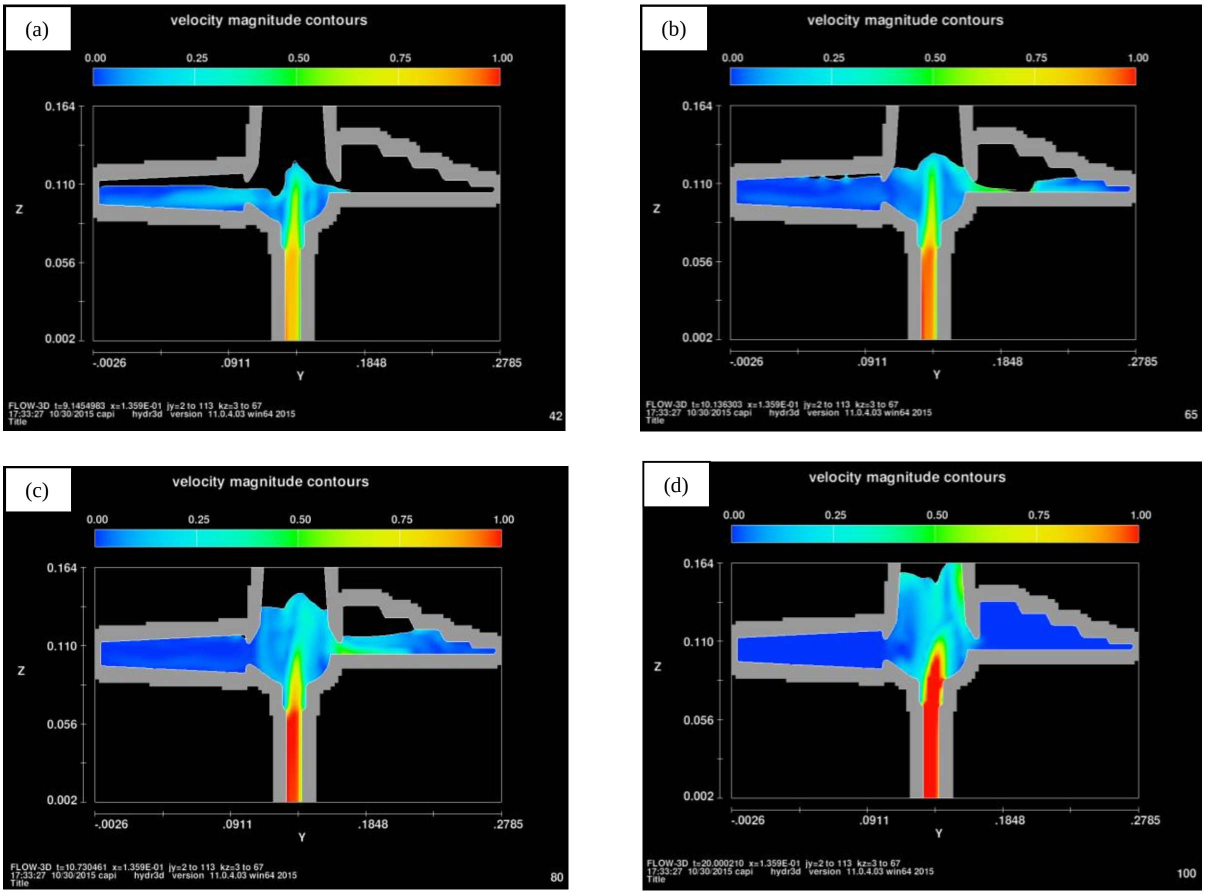

Figure 4.29 - Values of velocity magnitude contours for simulation of p-t (1): (a) values at 9.15s, (b) values at 10.14s, (c) values at 10.73s, (d) values at 20s

According to the result flux of the fluid (Figure 4.30), at 9s, into the simulation, it is visible that the flow through the conic geometry is prone to the creation of waves when the part is filling (Figure 4.30(a)). This also happens in the stair like geometry, but it is not problematic because the velocity is lower then $0.5\, m/s$, not being a turbulent regime. The waves origin is because of the impact of the molten metal in the mold walls, causing it to be deflected.

The creation of a vortex in the center of the part is also visible, since the beginning of the filling of the part, until the end. This happens as a result of the curvature of the base at the part (Figure 4.30(b)).

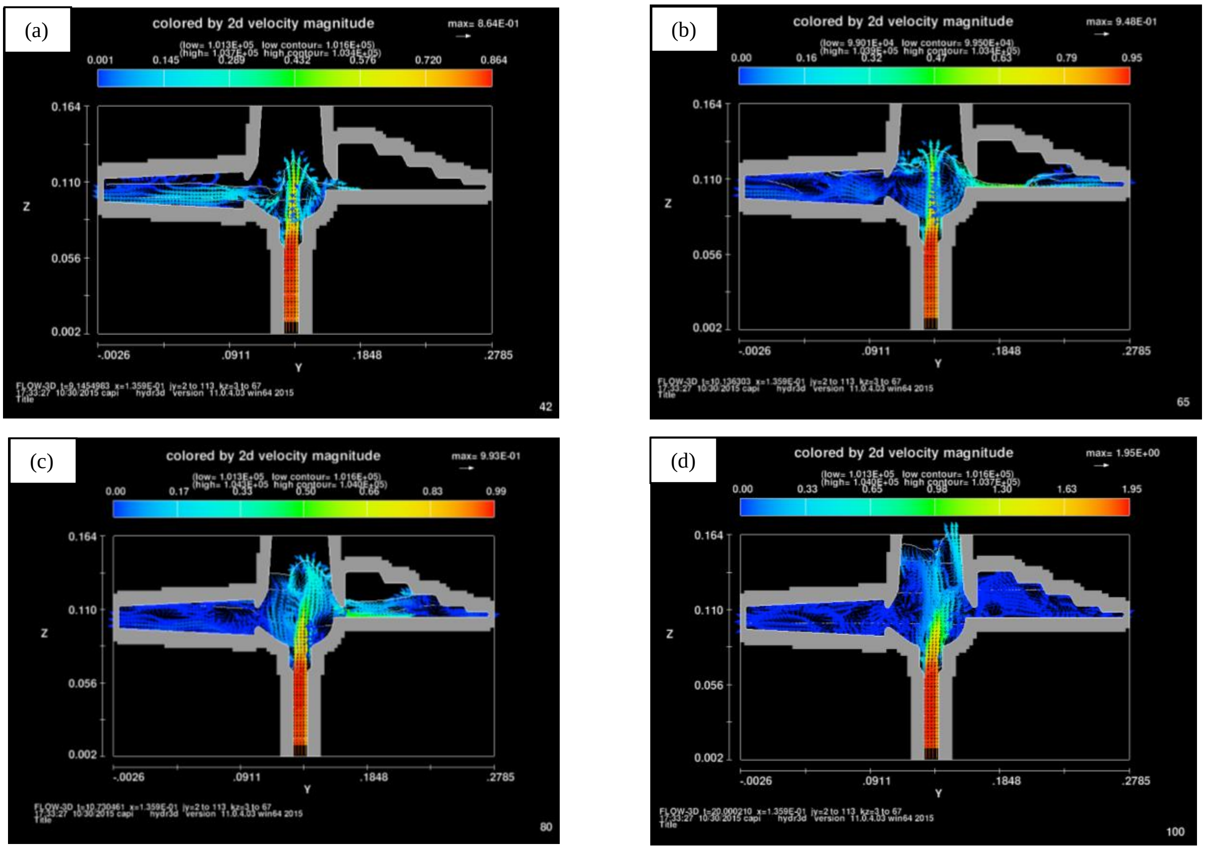

Figure 4.30 - Values of fluid flux for simulation of p-t (1): (a) values at 9.15s, (b) values at 10.14s, (c) values at 10.73s, (d) values at 20s

Although the pressure curve was having the desired results it was decided to test another pressure curve to confirm if there is any difference between simulations with different pressure curves. If the results were to be the same, means the simulation parameters need to be improved. This way the possibility of errors is refuted and validation of the parameters is made. For the pressure curve 2 the initial parameters used were (Table 4.5):

Table 4.5 - Initial conditions of simulation of pressure curve 2

Conditions	Values
Initial temperature of the fluid	700ºC
Pressure	Hydrostatic pressure
Initial pressure in the void	$1.01325e^{+5}$ Pa
Temperature in the void	25ºC
Cell size of the meshes	2.5
Alloy	Aluminum alloy A357
Molding sand	Furan Molding Sand Fine, CB 500 C
Gas	Air
Simulation approximately time	15s

At the end of the simulation, the fill fraction graph (Figure 4.31) shows that the time to fill the entire model was approximately 5.5s.

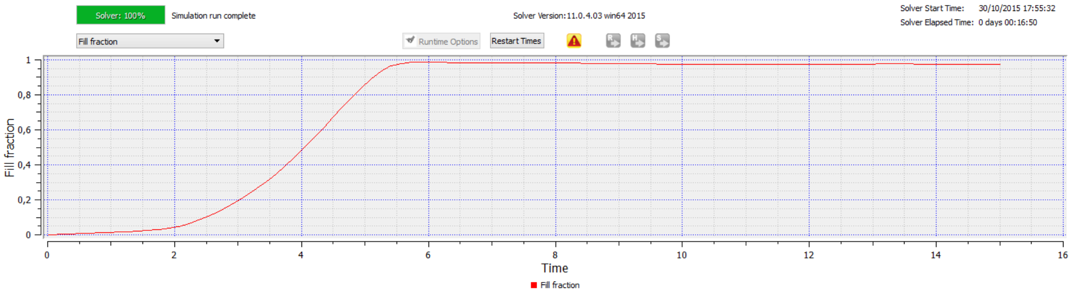

Solver: 100% Simulation run complete

Solver Version:11.0.4.03 win64 2015

Solver Start Time: 30/10/2015 17:55:32

Solver Elapsed Time: 0 days 00:16:50

Fill fraction
Runtime Options
Restart Times
1
0,8
0,6
0,4
0,2
0
Fill fraction
0
2
4
6
8
10
12
14
16
Time
Fill fraction

Figure 4.31 - Fill fraction pressure curve 2

The pressure curve for the simulation has 2 stages of pressure and it is as follows (Figure 4.32):

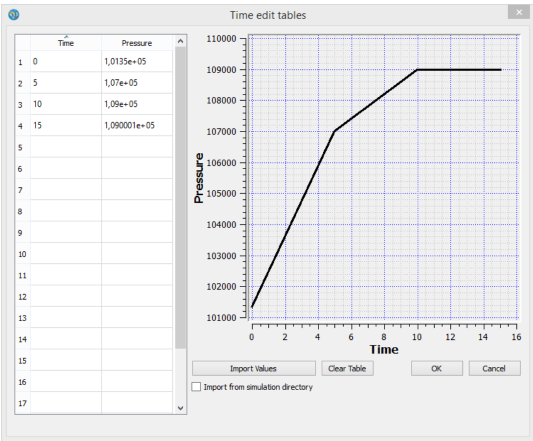

	Time	Pressure
1	0	1,0135e+05
2	5	1,07e+05
3	10	1,09e+05
4	15	1,090001e+05
5		
6		
7		
8		
9		
10		
11		
12		
13		
14		
15		
16		
17		

☐ Import from simulation directory

Time edit tables
110000
109000
108000
107000
106000
105000
104000
103000
102000
101000
Pressure
0
2
4
6
8
10
12
14
16
Time
Import Values
Clear Table
OK
Cancel

Figure 4.32 - Pressure curve 2

Concerning to the behavior of the pressure in the part (Figure 4.33), at approximately 4s it is higher at z min, with a value of $1.03429e^{+5}Pa$ and lower in the fluid that is in contact with the air, being at, $1.01282e^{+5}Pa$ (Figure 4.27(a)), which is similar to the simulation of the of pressure curve 1. At 4.4s (Figure 4.33(b)), the molten metal at the top, as it goes into contact with the mold, raises the pressure to $1.01339e^{+5}Pa$. It lowers through time, but maintains a certain pressure value due to the molten metal being in contact with the mold and the force made by the rising metal. In the middle of the part and at the end of the simulation (at 20s), the pressure registered has a value of $1{,}02639e^{+5}Pa$ (Figure 4.33(d)).

Pressures are lowering gradually, from z max to z min being the highest pressure at $1.03969e^{5}Pa$, located in the z min zone. The lowest pressure is $1.01309e^{+5}Pa$, at the top of the part. This pressure, in the z max, is a normal consequence because it is the zone connected to the atmosphere. Regarding the pressures and comparing with Figure 4.27, it is perceptible that the pressures are similar as both simulation start and end with the same values in the pressure curves. The biggest difference is in the way the geometry is being filled (Figure 4.33(c)), being more wavy in this case. Note the comparisons between simulations are made regarding the filling volume, since the simulations fill within different times.

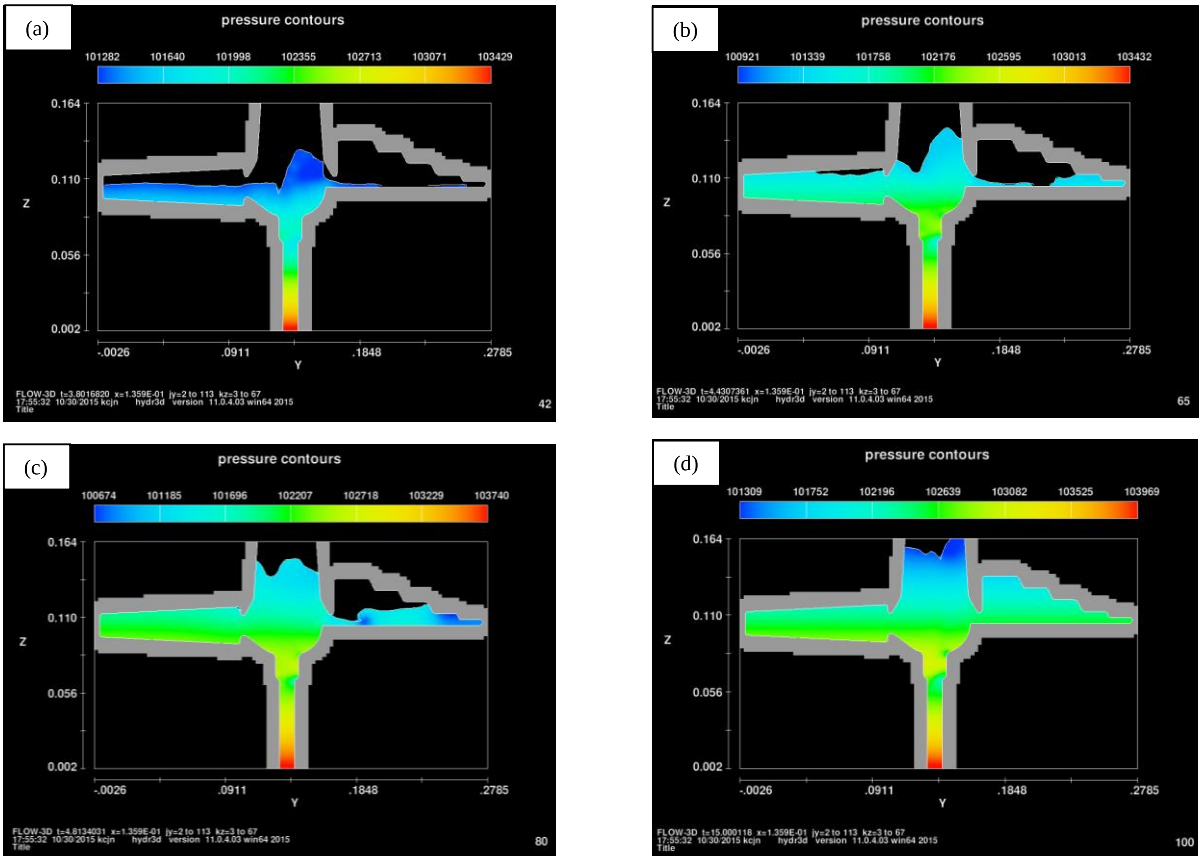

Figure 4.33 - Values of pressure contours for simulation of p-t (2): (a) values at 3.80s, (b) values at 4.43s, (c) values at 4.81s, (d) values at 15s

Analyzing the temperature simulation (Figure 4.34), it is noticeable that the behavior of the temperature is similar to the simulation of the pressure curve 1, with the temperatures being a bit higher in the beginning of the simulation, and lower at the end. The rising channel is the hottest zone, being initially 700ºC. The center of the part is around 650ºC (Figure 4.34(d)).

The cone geometry part is one of the zones that has the most heat dissipation, being the temperature around the 470ºC in the entrance of the metal and about 280ºC throughout the rest of the geometry. The stair like geometry has temperatures around 450ºC. The extremity of this zone is the one with the lowest temperature, because of it being thin, having temperatures around 197ºC.

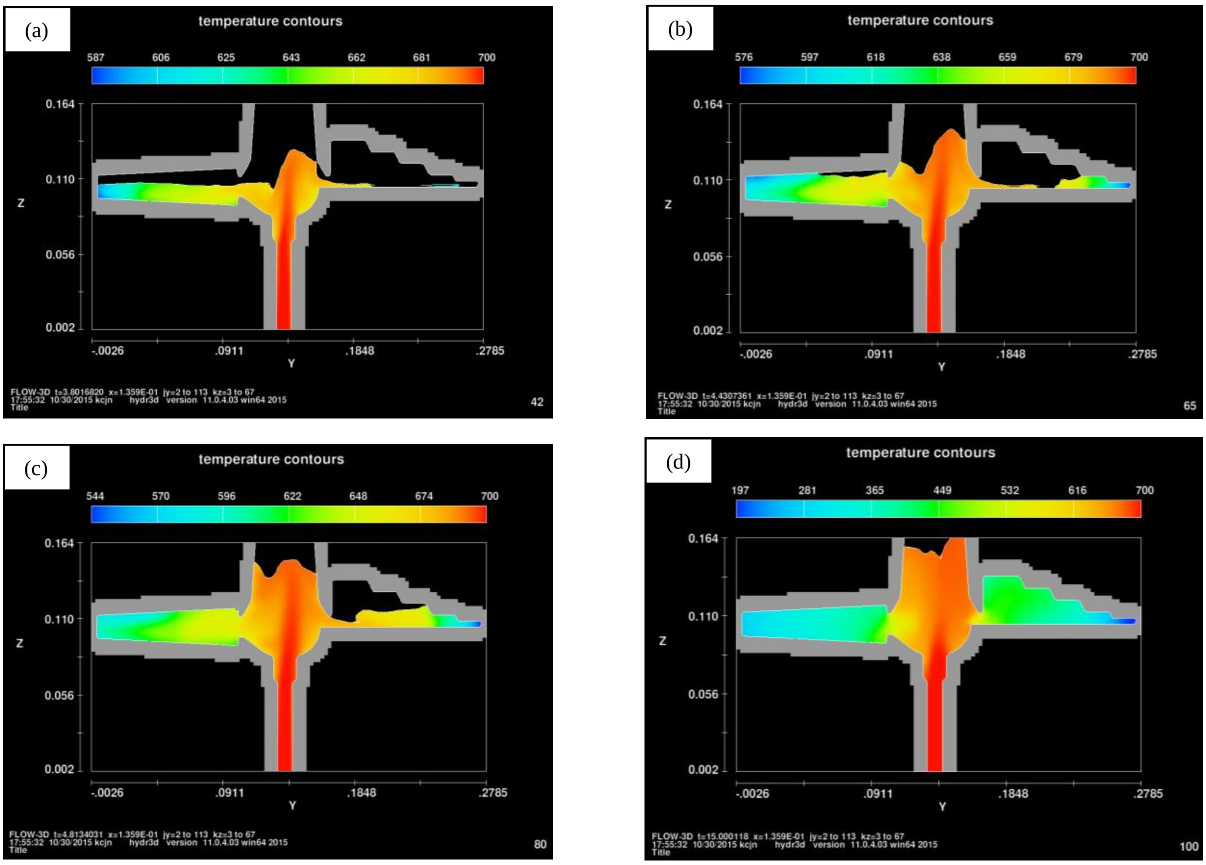

Figure 4.34 - Values of temperature contours using uniform component temperatures heat transfer parameter for simulation of p-t (2): (a) values at 3.80s, (b) values at 4.43s, (c) values at 4.81s, (d) values at 15s

In the simulation of the velocities (Figure 4.35), at approximately 4s (Figure 4.35(a)) the highest velocity is in the rising channel as in the simulation of pressure curve 1. However, in this simulation the velocity in the channel starts much higher, already at $1\,m/s$. It is noticeable that the center of the piece is more affected by the entry of the fluid, being the center zone always with $1\,m/s$. Comparing with the simulation of Figure 4.29, the fluid in this case has a more turbulent regime. It is also visible that the entrance of the stair like geometry is more problematic with this range of velocities, as the filling is more difficult, being the velocity near $0{,}75\,m/s$. The velocity in the cone part is $0\,m/s$ since the part is totally full (Figure 4.35(c)). The end of simulation is identical to the simulation of Figure 4.29 because the geometry is totally full, having the same velocities in the same spots.

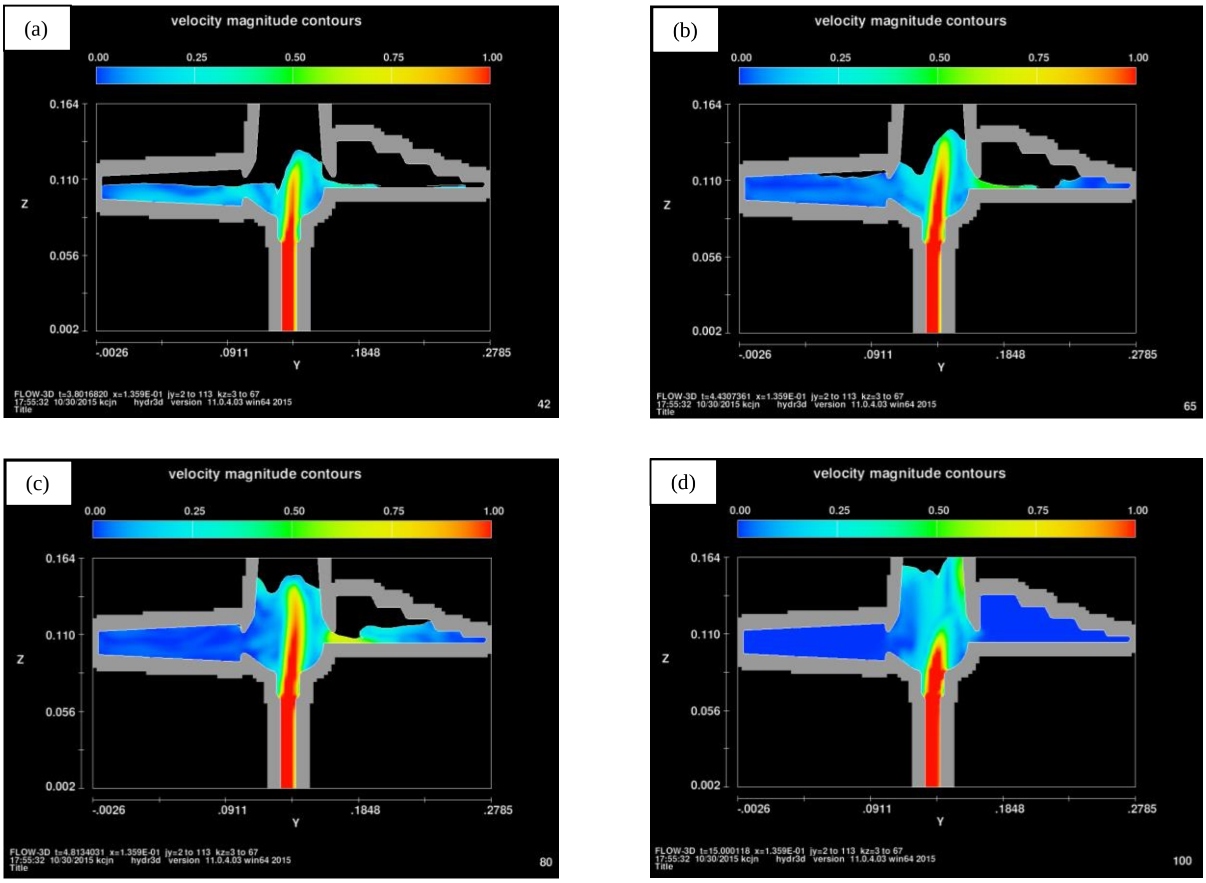

Figure 4.35 - Values of velocity magnitude contours for simulation of p-t (2): (a) values at 3.80s, (b) values at 4.43s, (c) values at 4.81s, (d) values at 15s

Observing the flux of the fluid (Figure 4.36), at 4s, into the simulation, it is visible that the fluid flow in the center of the piece is more dispersed, following the curvature of the piece (Figure 4.36(a)) later dispersing in the same zone (Figure 4.36(b)). In the conic geometry of Figure 4.30(a) a wavier flow, when comparing to Figure 4.36(a), is visible. This happens because of the timing of the simulation, which causes some noticeable flow waves, due to the impact between the fluid and the mold's wall, something not seen in this simulation considering that the figure shows simulation frame images. It is visible in Figure 4.36(c), that the flow in the center of the piece is more laminar then in Figure 4.30(c). This happens because of the air escaping through the stair like geometry, creating a vortex in the flow at the center of the piece. This is not visible in this simulation because the stair like geometry is not as full, taking more time for the air to escape.

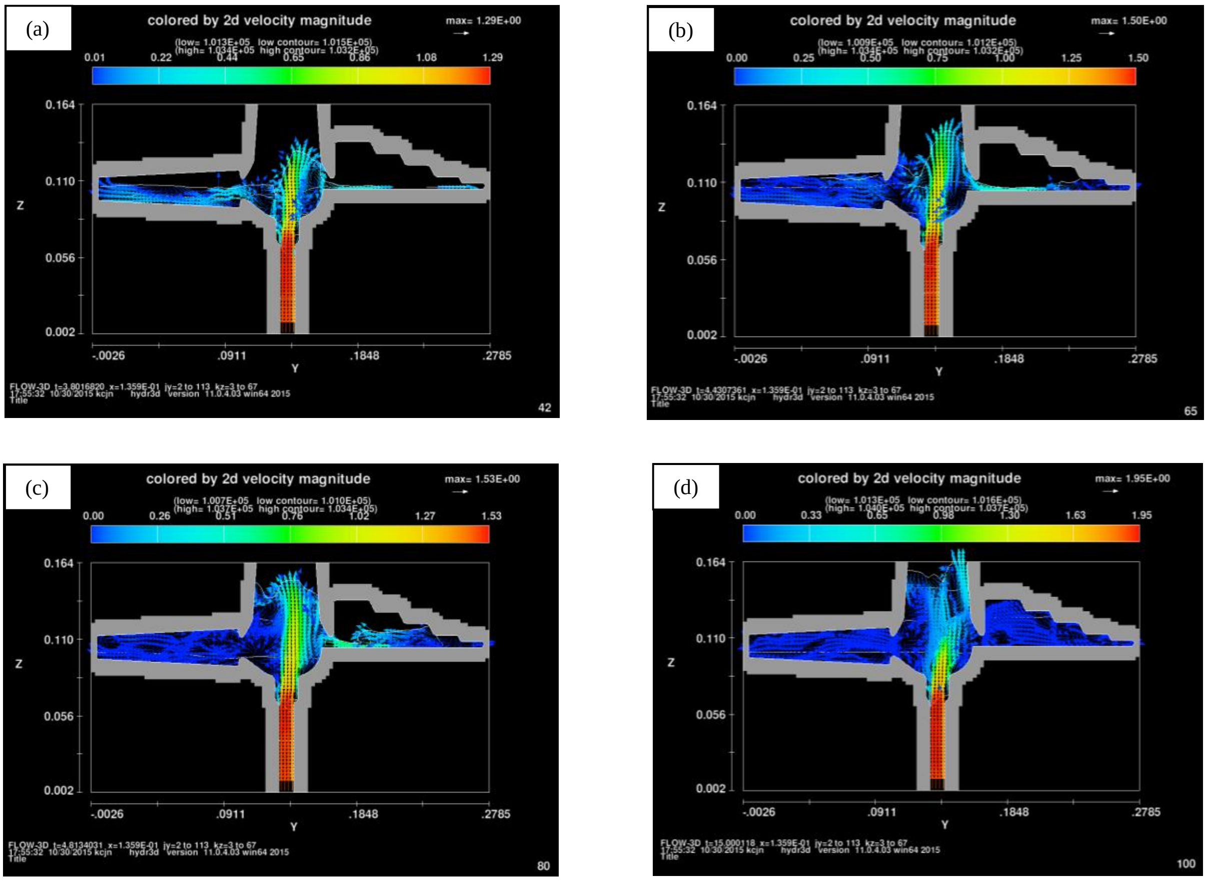

Figure 4.36 - Values of fluid flux for simulation of p-t (2): (a) values at 3.80s, (b) values at 4.43s, (c) values at 4.81s, (d) values at 15s

Considering both simulations it is possible to conclude that the injected pressure was lower than the pressures addressed in the bibliography. This is possible because of the geometry of the part. The information in the bibliography was achieved through practical experiments but with parts with different geometry, being the pressure values divergent.

According to the results regarding velocities it is observable that the velocities from pressure curve 1 are lower than those from pressure curve 2. The end of the rising channel is the most problematic zone. This problem does not affect significantly curve 1 because the fluid filling the part is still in a laminar regime. In curve 2, the flow is more turbulent, having a higher risk of jeopardizing the properties of the part. Comparing both simulations it is possible to conclude that a three stage pressure is more stable, having a more laminar regime than a two stage pressure.

Analyzing the flux simulation, the most problematic situation is the entry of the stair like geometry, visible after half of the simulation time, having some trouble in the flow of the fluid and expelling the air inside this zone. The small size of the entry makes it difficult for the air to go out and the fluid to go in, forming a vortex in the center of the part, producing a more turbulent flow of the fluid.

Concerning the temperature simulations, the values through time vary considerably, having a very rapid dissipation of heat better seen in the end of the simulations where it has a loss of around 300ºC of the lower temperature in a small space of time. Because of this a parameter was changed to obtain more realistic values. The heat transfer parameter was changed from uniform component temperatures to full energy (Figure 4.37).

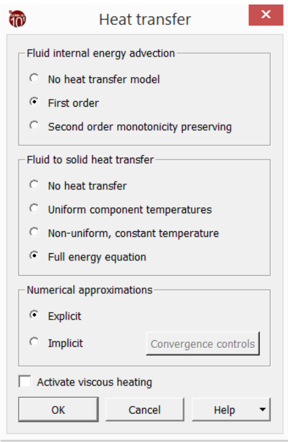

Heat transfer

Fluid internal energy advection
○ No heat transfer model
● First order
○ Second order monotonicity preserving

Fluid to solid heat transfer
○ No heat transfer
○ Uniform component temperatures
○ Non-uniform, constant temperature
● Full energy equation

Numerical approximations
● Explicit
○ Implicit

☐ Activate viscous heating

Figure 4.37 – New heat transfer parameters chosen to achieved temperatures validated with the bibliography

This allows the heat source to be distributed evenly over the component. The parameter that will be addressed next is the one that stands out for having the most significant changes. Firstly this parameter will be analyzed in the pressure curve 1.

Studying the temperature simulation (Figure 4.38), and comparing with the uniform component temperatures simulation it is perceptible that heat transfer is much lower in the full energy simulation. At approximately 9s the lowest temperature in this simulation (Figure 4.38 (a)) is of 624.3ºC contrarily to the uniform component temperatures simulation (Figure 4.28(a)) that are 100ºC lower. The behavior of the temperature in both simulations is similar in the first 3 times (Figure 4.38(a - c)).

The biggest difference is in the final situation, when the geometry is full. In the uniform component temperatures simulation (Figure 4.28 (d)) the lowest temperature goes to 214ºC having an interval of 486ºC between the lowest and the highest temperature. Results suggest that the difference, in the case of casting, is abnormal, justifying the need to change the heat transfer parameter to the full energy simulation. In the full energy simulation (Figure 4.38 (d)) the lowest temperature is 521ºC, having a difference of 179ºC from the highest. It is also visible in the full energy simulation that the temperature at the entry of the cone geometry is higher It stars at in the entry 640ºC and lowers gradually, as opposed to the case of the uniform component temperatures simulation, in which this geometry reaches 335ºC all around. Another difference is the center of the piece, that in full energy, the temperature is the same almost everywhere. In the uniform component temperatures simulation the temperature in this zone is around 619ºC.

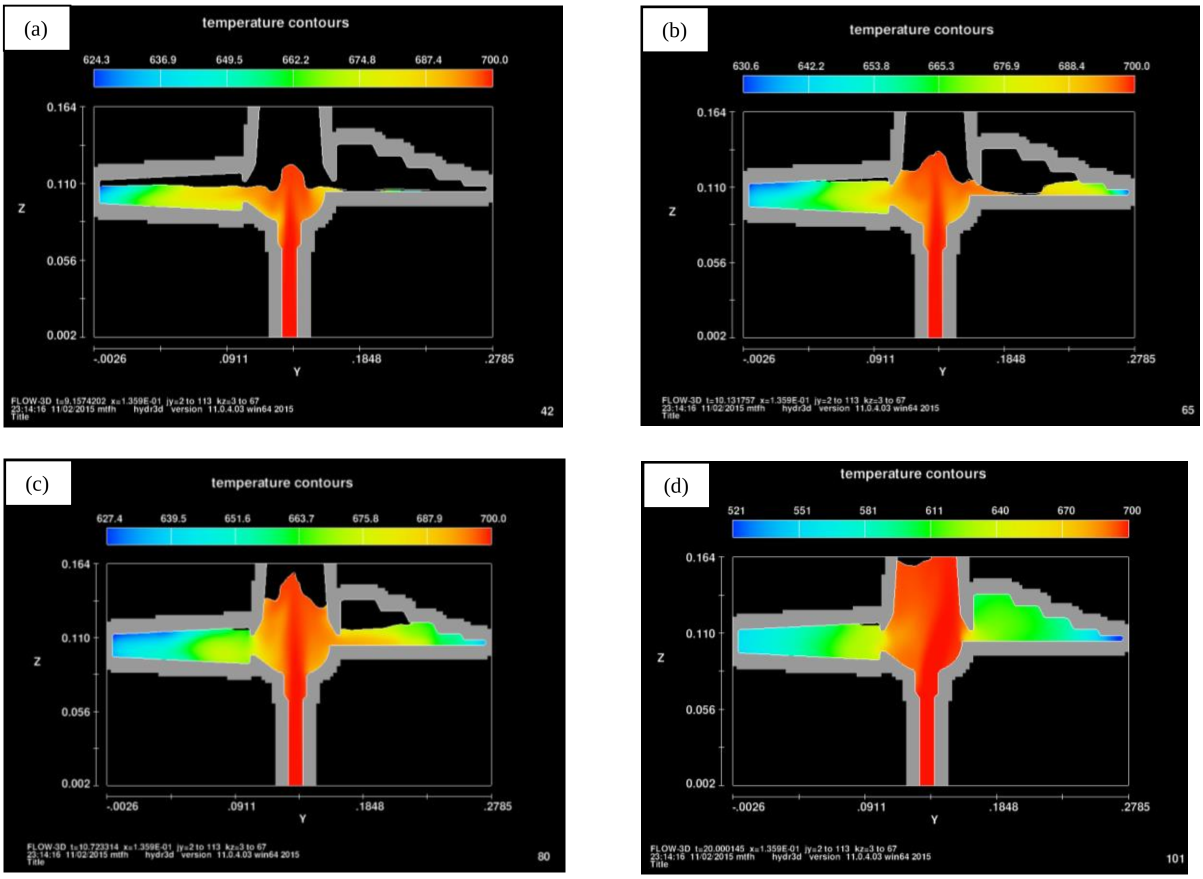

Figure 4.38 - Values of temperature contours using the full energy heat transfer parameter for simulation of p-t: (a) values at 9.15s, (b) values at 10.14s, (c) values at 10.73s, (d) values at 20s

Subsequent, the differences between the models resulting from different heat transfer parameters in pressure curve 2 will be explained. Comparing both simulations it is possible to see that the full energy simulation has the highest temperatures during all simulation, being the lowest temperature 628.6ºC, at 3.80s of simulation (Figure 4.39) and 587ºC in the case of the uniform component temperatures simulation it at the same time. The center zone of the piece, in the full energy simulation, is practically all the time near 700ºC. In the uniform component temperatures simulation the center zone is about 680ºC in the beginning (Figure 4.34(a)) and lowers to 650ºC.

The lowering of temperature in the cone geometry (Figure 4.39(c)) is more even in the full energy, dropping gradually at the top extremity, and then the greater part of the geometry is around 673ºC. In the uniform component temperatures simulation (Figure 4.34(c)) the difference of temperatures is much more noticeable being almost half of the geometry at 570ºC and the other half about 648ºC. Regarding the stair like geometry at 4.8s (Figure 4.39), the values for both simulations are similar.

At the end of simulation time in the full energy simulation, the cone geometry is gradually lowering its temperature, being 570ºC in the extremity and at the entry of the liquid 650ºC (Figure 4.39(d)). The uniform component temperatures simulation’s temperature in all this geometry is nearly the same being approximately 323ºC (Figure 4.34(d)). The behavior of the lowering of temperature is similar in both simulations regarding the stair like geometry. The lowest temperature is in the extremity of geometry in both simulations, however in the full energy simulation the value is 520ºC and in the uniform component temperatures simulation it is 197ºC.

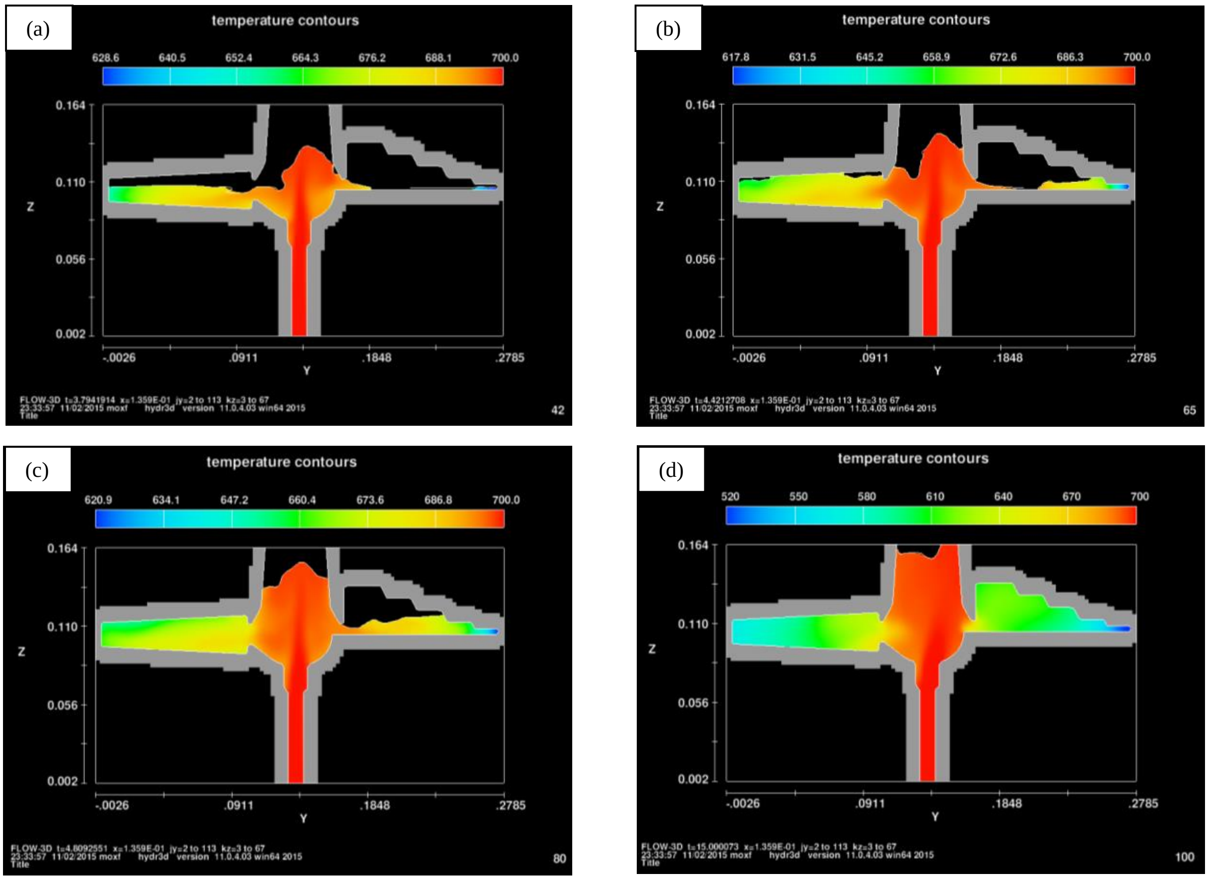

Figure 4.39 - Values of temperature contours using full energy heat transfer parameter for simulation of p-t (2): (a) values at 3.80s, (b) values at 4.43s, (c) values at 4.81s, (d) values at 15s

There is a big difference between values regarding the end of simulations, concluding that the uniform component temperatures simulations had a bigger loss of heat then the full energy. Comparing both heat parameters it is clear that the simulation that goes according to casting behavior regarding heat transfer is the one using the full energy, having a gradual amount of dissipation of heat.

4.5 Software simulation comparisions

Another software greatly used in the simulation of casting systems is the NovaFlow & Solid®. This software has a new pack where it is possible to use FVM in this simulation while the Flow 3D® uses FDM as explained in chapter 2.4. Because of this, a simulation of the same model and the same parameters in this software were used, to make a comparison between software (Figure 4.40). This way it is possible to validate the parameters in terms of simulation. In these simulations the complete casting system was used, including the reservoir and the crucible. Since the entire system is analyzed the pressure is applied on the molten metal surface. In the Flow 3D® simulation, the pressure was applied directly to the rising channel. The most important parameter to analyze on each software is the velocity of the simulations to evaluate the turbulence regime of the fluid.

Concerning the pressure curve 1 and comparing both simulations one can see the similarities of results from both software. In both cases the most problematic zone is in the end of the rising channel. In the simulation done in NovaFlow & Solid® this problem is more noticeable, reaching velocities equal or bigger then $0.5\,m/s$ while in the Flow 3D® the velocities are inferior. It is not a significant problem because it does not affect all the filling geometry causing the fluid to be turbulent, producing entrainment of the oxide films which causes a major casting failure.

Regarding to the pressure curve 2, the velocity in the simulation made on NovaFlow & Solid® is greater in all filling geometry then in Flow 3D®. Although a different flow chart there is a problem inherent in the end of the rising channel and in the middle of the piece, being in a more turbulent regime. Comparing both simulations of pressure curve 2 with 1, it is clear that curve 2 has the most turbulent flow regime.

As expected from the previous simulations on Flow 3D® the velocity in the pressure curve with 3 stages of pressure is more stable, having a laminar regime of fluid and thus being the most suitable for practical tests.

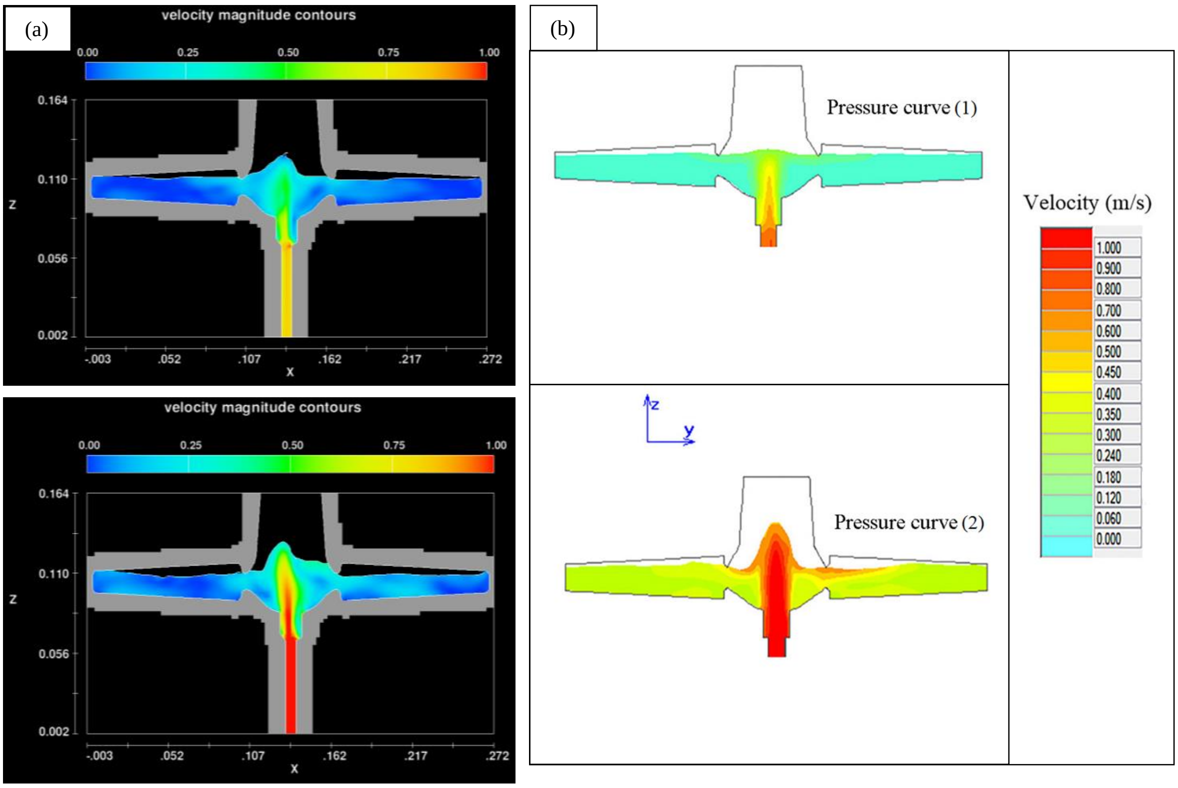

Figure 4.40 – Comparison between software simulations (a) Flow 3D® simulation,
(b) NovaFlow & Solid® simulation

5. CONCLUSIONS AND FUTURE PROSPECTS

Foundry industries have the need to offer products and services with increasingly better features, both appealing and functional. Modernization is the key to improve casting quality and productivity. Due to the introduction of computers in foundries it has been possible to minimize manufacturing time, assuring the final quality of the components, which leads to a great saving of production resources, both at the level of the associated costs and equipment maintenance, having as consequence a satisfied customer. This chapter intends to present the conclusions of this dissertation.

5.1 Conclusion

The work presented in this dissertation has a starting point in the low pressure cast process. The process consists in applying pressure to the molten metal until it rises, filling the wanted part. One of the most important advantages is the control of the injected pressure, in order to control the velocity of the metal and attaining and laminar flow regime, avoiding entrainment of the oxide films which causes major damage to the castings

To study this process the Flow 3D® software was chosen, governed with finite difference method, one of the most popular methods used in numerical simulation due to its accuracy and simplicity. For the simulations two geometrical models were created. One containing the full system, consisting of the crucible, the reservoir, rising channel and the part. While the other one was only the part. Two models were developed because, after simulating the complete one, some errors occurred, and to reduce the error likelihood of the geometric model, it was chosen to simulate only with the final part. The initial parameters were chosen resorting to the existing bibliography and preliminary practical trials in previous works. Then the rest of the parameters were selected using the same method and when they weren't found it was used an iteration method.

When the simulation was fully functional two pressure curves were used. The first analyzed has three stages of pressure while the second has two. Regarding the injected pressure it was possible to use lower pressures then the pressures addressed in the bibliography. The most plausible reason is the different geometry. The values achieved in the available bibliography were obtained by using parts with different geometries, making it possible for the theoretical values to vary. Just like the situation mentioned above, some practical experiments were made in order to achieve these values but since the geometries are different, they might not be suited.

About the temperature simulations, the values through time vary considerably, having a very rapid dissipation of heat better seen in the end of the simulations where it has a loss of around 300ºC of the lower temperature in a small space of time. Another simulation was made, changing the parameter of heat transfer. With these changes the variation of the lowest temperature, in the same amount of time, was of 100ºC, making this a more plausible output. These changes didn’t interfere in a relevant way regarding the other output parameters.

Concerning the velocities it is noticeable that the velocities from pressure curve 1 are lower than those from pressure curve 2. The most problematic zone is in the end of the rising channel, not being relevant to curve one because it doesn’t affect much of the fluid filling the part. In curve 2, the flow is more turbulent, having a higher risk of jeopardizing the properties of the part. Comparing both simulations it is possible to conclude that a three stage pressure is more stable, having a more laminar regime than a two stage pressure.

Analyzing the flux simulation it is visible that the most problematic zone is the entry of the stair like geometry, occurring in the middle of the simulation, having some trouble in the flow of the fluid and expelling the air inside this zone. The small size of the entry makes it difficult for the air to escape and the fluid to enter, forming a vortex in the center of the part, producing a more turbulent flow of the fluid. To solve this problem the CAD model should be redesigned creating a bigger path.

As previously said, in the end of this dissertation a comparison between the simulations achieved in Flow 3D® with others made in NovaFlow & Solid® was made. The main difference between the simulations was that the one with NovaFlow & Solid® was made with the complete casting system. It was visible that the simulations were very similar, validating the simulations, reaching and corroborating the analysis made in Flow 3D simulations.

5.2 Future Prospects

For future prospects it is proposed to change the CAD model regarding the entry in the stair like geometry. This path must be enlarged to induce a smoother flow of metal.

Another pertinent contribution would be to the study of the solidification process. To this end, two main lines of work would be necessary: analyzing the stabilization pressure to prevent shrinkage in order to produce the casted part; and studying the amount of time needed to achieve the solidification of the part, to then lower the pressure so that blockage of the rising channel doesn’t occur. This part of the process will focus on the energetic physical models.

Also, another useful work would be to pursue practical validation using the casting of the piece and making a comparative analysis of the data obtained in the simulation with the data regarding the casting. This way it is possible to visualize the accuracy of the simulation and to improve the parameters if the practical results do not coincide with the simulation.

BIBLIOGRAPHY

[1] E. Stanley and D. B. Sc, “Fluid Flow Aspects of Solidification Modelling : Simulation of Low Pressure Die Casting .”

[2] Y. Sahin, “Computer aided foundry die-design,” *Metallography*, vol. 24, no. 8, pp. 671–679, 2003.

[3] F. Bonollo, J. Urban, B. Bonatto, and M. Botter, “Gravity and low pressure die casting of aluminium alloys : a technical and economical benchmark,” *La Metall. Ital.*, vol. 97, no. 6, pp. 23–32, 2005.

[4] P. a and R. R, “Study of the effect of process parameters on the production of a non-simmetric low pressure die casting part,” *La Metall. Ital.*, pp. 57–63, 2009.

[5] “Fundição em baixa pressão | Aluinfo.” [Online]. Available: http://www.aluinfo.com.br/novo/materiais/fundicao-em-baixa-pressao. [Accessed: 18-Sep-2015].

[6] “Low Pressure Sand Casting by Wolverine Bronze.” [Online]. Available: http://www.wolverinebronze.com/low-pressure-sand-casting.php. [Accessed: 18-Sep-2015].

[7] A. Reikher, “Numerical Analysis of Die-Casting Process in Thin Cavities Using Lubrication Approximation,” no. December, 2012.

[8] P. Fu, A. a. Luo, H. Jiang, L. Peng, Y. Yu, C. Zhai, and A. K. Sachdev, “Low-pressure die casting of magnesium alloy AM50: Response to process parameters,” *J. Mater. Process. Technol.*, vol. 205, no. 1–3, pp. 224–234, 2008.

[9] X. Li, Q. Hao, W. Jie, and Y. Zhou, “Development of pressure control system in counter gravity casting for large thin-walled A357 aluminum alloy components,” *Trans. Nonferrous Met. Soc. China*, vol. 18, no. 4, pp. 847–851, 2008.

[10] J. a. Hines, “Determination of interfacial heat-transfer boundary conditions in an aluminum low-pressure permanent mold test casting,” *Metall. Mater. Trans. B*, vol. 35, no. 2, pp. 299–311, 2004.

[11] A. Lima, A. Freitas, and P. Magalhães, “Processos de vazamento em moldações permanentes,” pp. 40–49, 2003.

[12] Y. B. Choi, K. Matsugi, G. Sasaki, K. Arita, and O. Yanagisawa, “Analysis of Manufacturing Processes for Metal Fiber Reinforced Aluminum Alloy Composite Fabricated by Low-Pressure Casting,” *Mater. Trans.*, vol. 47, no. 4, pp. 1227–1231,

2006.

[13] G. Mi, X. Liu, K. Wang, and H. Fu, “Numerical simulation of low pressure die-casting aluminum wheel,” *China Foundry*, vol. 6, no. 1, pp. 48–52, 2009.

[14] J. Kuo, F. Hsu, and W. Hwang, “ADVANCED Development of an interactive simulation system for the determination of the pressure ± time relationship during the ® lling in a low pressure casting process,” vol. 2, pp. 131–145, 2001.

[15] S.-G. Liu, F.-Y. Cao, X.-Y. Zhao, Y.-D. Jia, Z.-L. Ning, and J.-F. Sun, “Characteristics of mold filling and entrainment of oxide film in low pressure casting of A356 alloy,” *Mater. Sci. Eng. A*, vol. 626, pp. 159–164, 2015.

[16] “Casting Training Class - Lecture 10 - Solidification and Shrinkage-Casting.” FLOW-3D®.

[17] “UAB Casting Engineering Laboratory.” [Online]. Available: file:///C:/Users/Jos%C3%A9 Belo/Desktop/Artigo_Software/UAB Casting Engineering Laboratory.htm. [Accessed: 09-Nov-2015].

[18] A. Louvo, “Casting Simulation as a Tool in Concurrent Engineering,” pp. 1–12, 1997.

[19] T. R. Vijayaram and P. Piccardo, “Computers in Foundries,” vol. 30, 2012.

[20] M. Sadaiah, D. R. Yadav, P. V. Mohanram, and P. Radhakrishnan, “A generative computer-aided process planning system for prismatic components,” *Int. J. Adv. Manuf. Technol.*, vol. 20, no. 10, pp. 709–719, 2002.

[21] Ministry_of_Planning, “Digital Data,” vol. 67, pp. 1–6, 2004.

[22] S. Shamasundar, D. Ramachandran, and N. S. Shrinivasan, “COMPUTER SIMULATION AND ANALYSIS OF INVESTMENTCASTING PROCESS.”

[23] J. M. Siqueira and G. Motors, “Simulation applied to Aluminum High Pressure Die Casting,” pp. 1–5, 1998.

[24] C. Fluid, *COMPUTATIONAL FLUID DYNAMICS*. Abdulnaser Sayma & Ventus Publishing ApS, 2009.

[25] C. a. Felippa, “1 - Overview,” *Adv. Finite Elem. Methods*, pp. 1–9.

[26] a. Meena and M. El Mansori, “Correlative thermal methodology for castability simulation of ductile iron in ADI production,” *J. Mater. Process. Technol.*, vol. 212, no. 11, pp. 2484–2495, 2012.

[27] T. R. Vijayaram, S. Sulaiman, a. M. S. Hamouda, and M. H. M. Ahmad, “Numerical simulation of casting solidification in permanent metallic molds,” *J. Mater. Process.*

Technol., vol. 178, pp. 29–33, 2006.

[28] “General CFD FAQ -- CFD-Wiki, the free CFD reference.” [Online]. Available: http://www.cfd-online.com/Wiki/General_CFD_FAQ. [Accessed: 10-Nov-2015].

[29] “FEM | FEA | CFD.” [Online]. Available: http://fem4analyze.blogspot.pt/. [Accessed: 09-Nov-2015].

[30] “Fundição; revista da Associação portuguesa de fundição,” *Fundição*, vol. N^{o} 227.

[31] “Casting Training Class - Lecture 1 - Introduction_to_FLOW-3D - Casting.” FLOW-3D®.

[32] F. Science, “FLOW-3D Cast Documentation,” no. 3.5, p. 80, 2012.

[33] “Casting Training Class - Lecture 4 - Geometry Building - General.” FLOW-3D®.

[34] F. Science, “FLOW-3D v11.0.3 User Manual,” pp. 1–132, 2015.

[35] “Casting Training Class - Lecture 5 Meshing Concept - General.” FLOW-3D®.

[36] “Casting Training Class - Lecture 6 - Boundary_Conditions - Casting.” FLOW-3D®.

[37] “Casting Training Class - Lecture 9 - Physical Models-castings.” FLOW-3D®.

[38] P. A. D. Jácome, M. C. Landim, A. Garcia, A. F. Furtado, and I. L. Ferreira, “The application of computational thermodynamics and a numerical model for the determination of surface tension and Gibbs–Thomson coefficient of aluminum based alloys,” *Thermochim. Acta*, vol. 523, no. 1–2, pp. 142–149, 2011.

[39] J. P. Anson, R. A. L. Drew, and J. E. Gruzleski, “The surface tension of molten aluminum and Al-Si-Mg alloy under vacuum and hydrogen atmospheres,” *Metall. Mater. Trans. B Process Metall. Mater. Process. Sci.*, vol. 30, no. 6, pp. XVI–1032, 1999.

ATTACHMENT I – BOUNDARY CONDITIONS

Wall boundary conditions: are similar to symmetry conditions in which the mass flux across the boundary is not permitted. Also, it does not allow specifying the roughness on wall borders. However, heating and viscosity voltages can be applied contrarily to the symmetric boundary [32,34,36].

Continuing boundary conditions: The gradients of all flow parameters in the direction normal to the boundary are set to zero, resulting in the continuative boundary condition. The zero-derivative condition is intended to represent a smooth continuation of the flow across the boundary. If the flow tries to enter the computational region through this kind of boundary, it will do it starting from of a condition of zero speed (stagnation). In addition, the height of fluid surface at the free surface flow can be set at any of four boundaries of the mesh, the left (low x), right (high X), front (lower y) and backward (high y). The height of the surface is only applied if the fluid is entering the domain through an outflow boundary. In Figure A1.1 there's a representation of this model [32,34,36].

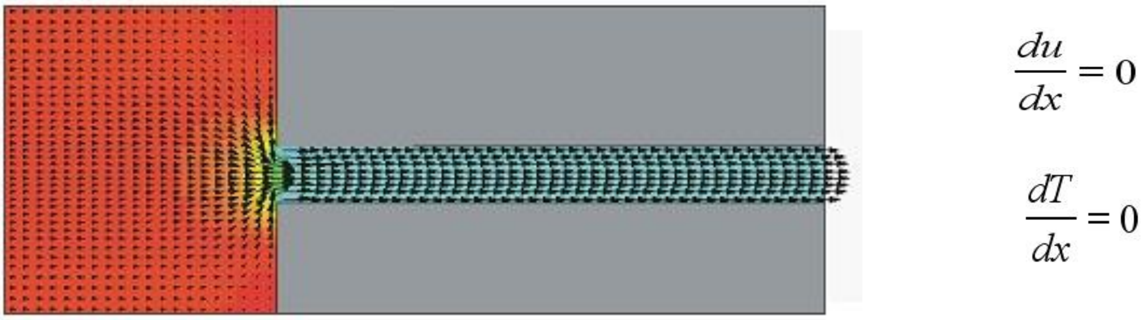

Assumes u, T, μ, and pressure do not change in flow direction

Figure A1. 1 - Fluid entering the domain through an outflow boundary [36]

Velocity boundary conditions: This type of boundary sets a velocity condition in the applied directions. The velocity may be constant or time dependent. Dependent boundaries of time are obtained by linear interpolation between the set values [32,34,36].

Volume flow rate boundary conditions: Can be applied to any boundary of the mesh. These conditions are governed by three characteristics, namely [32,34,36]:

- Being the flow rate specified, no fluid height and without a defined direction, the flow is distributed over the open area of the boundary and the flow direction is normal to the boundary.
- Being the flow rate and fluid height specified, the flow is distributed over the 'wet' area of the border and the flow direction is normal to the boundary.
- And when the flow rate, the fluid height and the direction are specified, the flow is distributed over the 'wet' area of the boundary and the direction of this will be in accordance with a specification.

Outflow boundary condition: Allows the flow to exit the domain without reflecting back into the domain. Waves and disturbances leave the domain without any problems and the height of the fluid or any other variable flow on this border are not set [32,34,36].

ATTACHMENT II – BOUNDARY CONDITIONS OF SIMULATION

The boundary conditions that were used were symmetric except in the air entry zone (Figure A2.1), wherein the pressure in the air inlet region is characterized by its increase from $1{,}0135e^{5}\ Pa$ (atmospheric pressure) to $1{,}114575e^{5}Pa$ in 5 s interval maintaining this value until 20s. When the mold is full the pressure is maintained till the solidification cycle ends.

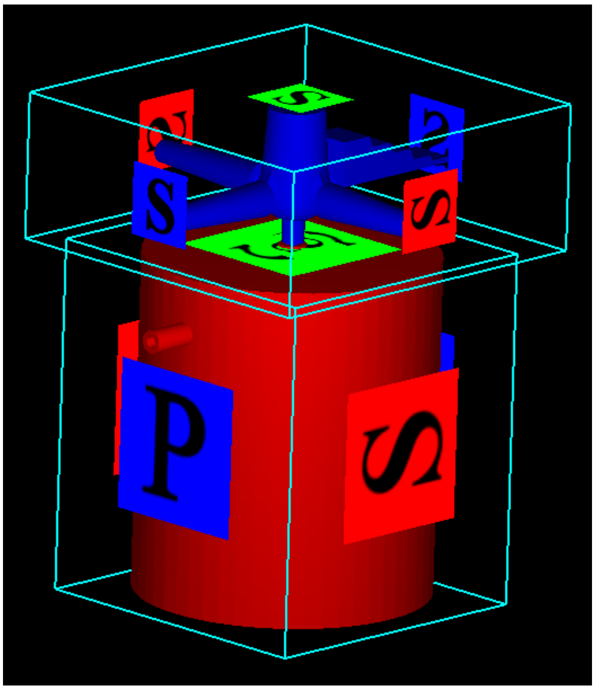

Figure A2. 1 - Boundary conditions of simulation